european space agency
agence spatiale européenne

AN ASSESSMENT OF ERS SAR LOW RESOLUTION IMAGERY

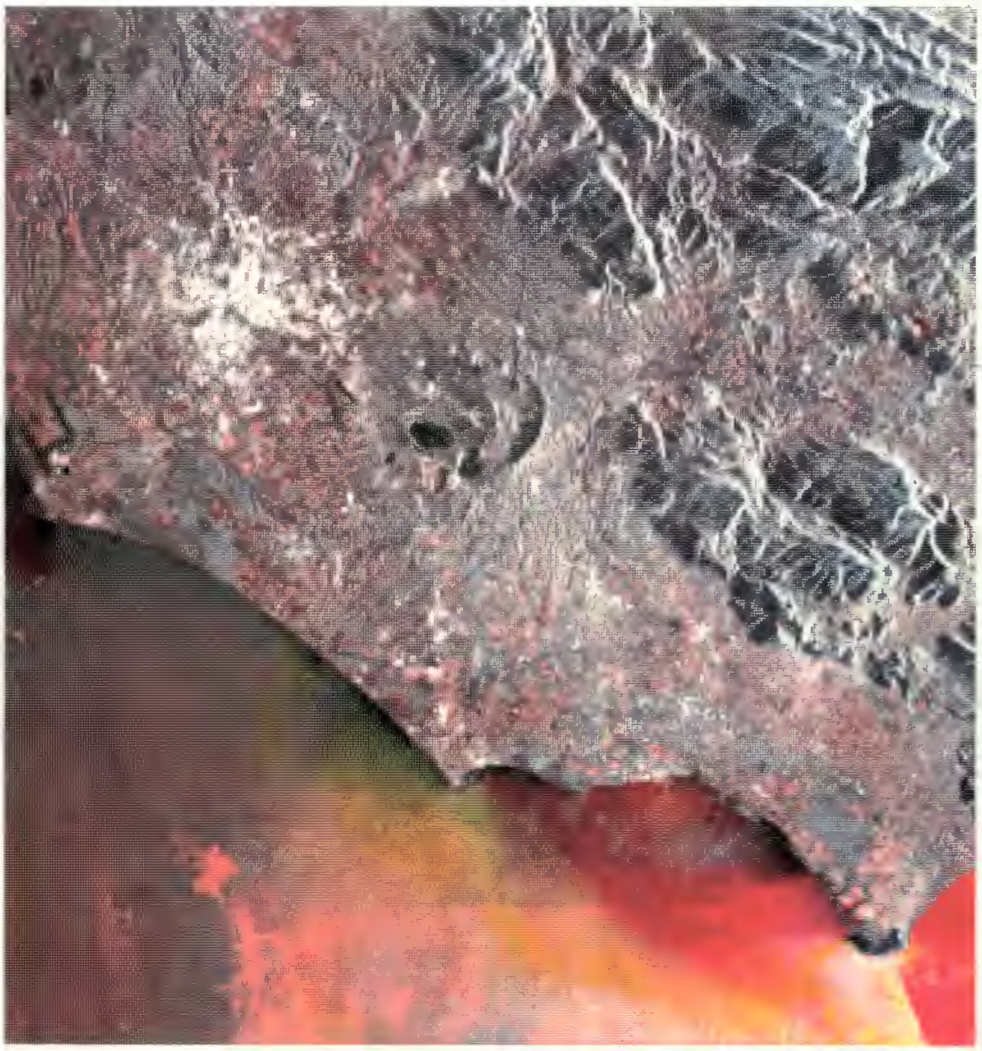

G. SOLAAS
H. LAUR

PROJECTS & ENGINEERING DEPARTMENT
EARTH OBSERVATION DIVISION
ERS MISSIONS SECTION

ES-TN-DPE-OM-GS01, version 1.1 *July 1993*

Gaute Aa. Solaas contribution to the technical note was done under an ESA Fellowship at ESRIN.

Cover Picture

Multitemporal ERS-1 Low Resolution Image of Rome

The cover image is a multitemporal presentation of three ERS-1 low resolution images (derived from PRI products). It is located over Rome, Italy, and the images were captured during January 1992.

The short time span between the images results in only small changes over land, while the wind patterns over the sea have changed significantly. Note that the outlet of the river Tiber has a consistently low backscatter on the three dates.This is probably due to pollution in the water.

Only mean preserving and continuous transformations have been applied, which is necessary for multitemporal use. In such an image, the colors are meaningful and allow a quick interpretation of the backscattering levels change. For example the reddish color over land means that the backscattering is higher for the "red date" than for the two other dates. Indeed, for this particular date the fields are wet due to rainfall, which significantly increases their backscattering coefficients.

If an histogram equalization had been applied to each low resolution image, then the multitemporal interpretation would have been difficult, if not impossible to perform with accuracy.

Acronyms and Abbreviations

ACS	Advanced Computer Systems
ASF	Alaska Station Facility
CCRS	Canada Centre for Remote Sensing
DLR	Deutsche Forschungsanstalt für Luft und Raumfahrt
DN	Digital Number
ECISAR	ERS 1 SAR Calibration and Quality Analysis Group
ENL	Equivalent Number of Looks
FD	Fast Delivery
FRI	TSS ERS Full Resolution Image
HR	High Resolution
INPE	Instituto de Pesquisas Espaciais
IRF	Impulse Response Function
LR	Low Resolution
LRI	TSS ERS Low Resolution Image
MCS	Matra Cap Systemes
MDA	MacDonald Dettwiler
NRCT	National Research Council of Thailand
PSLR	Peak to Sidelobe Ratio
PRI	ESA ERS Precision Image
SAR	Synthetic Aperture Radar
SARCALQ	ESRIN SAR-Calibration and Quality Control System
SGC	CCRS ERS SAR Georefenced Coarse Resolution Image
SGF	CCRS ERS SAR Georefenced Fine Resolution Image
SLC	ESA ERS Single Look Complex Product
SPECAN	Spectral Analysis
TSS	Tromsø Satellite Station
UI16	ESA ERS Fast Delivery Image
UILR	ESTEC ERS-1 Low Resolution SAR Image
VMP	Verification Mode Processor

Contents

1 INTRODUCTION

The objective of the technical note is to describe and to analyse the various concepts associated with the ERS SAR low resolution imagery. This study is done in order to evaluate a range of products, to consider the trade-offs involved in product specification and to propose some recommendations for low resolution imagery of quality suitable for a broad range of potential applications.

In chapter 2 we give an overview on the concepts associated with SAR low resolution imagery. We explain the main trade-offs in SAR low resolution imagery. We then describe the techniques used during the generation of low resolution imagery with focus on the techniques for the data conversion from 16 to 8 bits.

In chapter 3 we investigate the quality of the existing ERS SAR low resolution products derived from high resolution products. For some of the analysed products, we propose quality improvements.

In chapter 4 we investigate the quality of the existing ERS SAR low resolution imagery directly derived from the raw data.

In chapter 5 we simulate different levels of speckle reduction in low resolution imagery. The simulated images are generated to demonstrate varying image quality.

Finally, in the conclusion, we make some recommendations for ERS SAR low resolution product specifications and give our view on the likely evolution of this kind of imagery.

2 Introduction to Low Resolution SAR Imagery

A major reason to produce low resolution images is to reduce data volume and thereby to reduce time of data distribution. Another important reason for low resolution imagery generation is the possibility to make visible the ERS SAR acquisitions, i.e. the possibility to 'see' all acquired raw data.

Furthermore SAR low resolution imagery would :

1. facilitate scientific studies and surveillance applications of large scale phenomena (mainly in oceanography, sea ice kinetics and geology),
2. promote the use of high resolution data (browse function, i.e. identification of scenes to be processed at high resolution),
3. allow a closer surveillance of the SAR instrument performances.

In the case of the ERS SAR data, the term 'low resolution image' is commonly used to refer to an image with spatial resolutions ranging from 100 to 200 metres.

According to its origin, the ERS-1 SAR low resolution imagery available today falls into two categories: LR imagery derived from high resolution products and LR imagery derived from raw data.

A. *LR imagery derived from High Resolution products*:

Such imagery is derived from standard high resolution products (e.g. UI16 and PRI) by different techniques commented in the following chapter. At present such imagery is used for two different purposes:

- to provide scientific users with a ***digital product*** for studies of large scale phenomena. Such a product, usually called 'low resolution product', has a good radiometric resolution (usually more than 30 effective looks) and can potentially be absolute calibrated,

- to provide application users (real-time availability) and archive data centres (browse or quick-look) with a photo or screen ***display*** of the available HR products. Usually such images are generated with contrast enhancement and further data volume reduction (in comparison with the previous case). It should be noticed that screen display can be generated either from HR products or LR products.

The resulting outputs of these two purposes (digital product and screen display) are opposite because contrast enhancement and strong data reduction mean always radiometric degradation.

The major disadvantage of the LR imagery derived from HR imagery is its ***limited access*** caused by the limited generation of HR products. Within the ESA ground segment (Kiruna, Fucino and Maspalomas ground stations) ***more than 85 % of the raw data acquired have never been processed to HR products***. Although this value is large, one should not underestimate the amount of HR products already processed within the ESA ground segment : at mid-June 1993, about 23 000 standard frames (incl. double acquisition), i.e. 230 millions km^2 (Earth surface = 510 millions km^2) !

In chapter 3 we review existing LR imagery derived from HR products.

B. LR imagery directly derived from raw data :

Such imagery is derived directly from the acquired raw data. At present such imagery has one purpose:

- to provide archive data centres (browse) with a photo or screen ***display of 100 % of the acquired raw data***. Usually such images are generated as standard frames cut out of a strip corresponding to a whole SAR segment. It is mainly used to assist users in the choice of HR production requests. As previously such imagery can also be used for real-time applications.

To reach this goal (processing of 100 % of the raw data), the processing time of such imagery shall be very short (better than $1/8^{th}$ real time).

The major disadvantage (up to now) of the LR imagery derived from raw data is its ***poor radiometric resolution*** (usually less than 10 effective looks). This means that such an image cannot be used as a digital product for users.

However the potential exists to improve radiometric resolution without losing processing time. ***This is the main improvement to be expected in LR imagery generation for the next years*** . A near real-time image with good radiometric resolution (more than 30 effective looks) could result in a digital product suitable for users and covering all ERS SAR acquisitions.

In chapter 4 we review existing LR imagery derived from raw data.

2.1 Trade-Offs

Several factors must be traded off against each other in the generation of low resolution SAR imagery :

2.1.1 Spatial resolution against image size

The more coarse the spatial resolution one uses, the smaller is the volume of data per image. The problem with the distribution of high resolution products is their size, which for many users implies that tapes must be sent physically to their location. Generally the data volume decreases as the inverse square of the spatial resolution.

Reduced data volume implies reduced pixel size and by consequence reduced spatial resolution. There is however a lower limit since even large scale phenomena have a characteristic spatial sampling limit. A study of the viable applications and specific spatial resolution requirements is needed if LR imagery has to be used as digital LR product. The consensus of about 100 m pixel size (i.e. about 150 m spatial resolution) has to our knowledge not been based on such a survey. For display purposes (i.e. browsing or real-time dissemination) the dominant consideration is the data volume (less than 250 Kbytes); it means that pixel size reduction (about 200 m) or data compression are required.

Figures 2.1 to 2.3 illustrate the trade-off between radiometric and spatial resolutions that is possible to obtain when deriving LR imagery from three different ERS-1 HR products, namely the SLC (Single Look Complex), PRI (Precision Image) and UI16 (Fast Delivery Image) products [Ref. 1]. For each product the ground range resolution cell area has been calculated (SLC : 5 x 25 = 125 m^2, PRI : 22 x 25 = 550 m^2 and UI16 : 25 x 28 = 700 m^2). The equivalent number of looks NL for any simulated spatial resolution is then found by taking the ratio between the simulated and the original resolution cell and multiplying by the number of looks in the original image:

$$NL_{new} = NL_{original} \times (\text{resolution cell area})_{new} \;/\; (\text{resolution cell area})_{original}$$

The three figures represent different intervals of spatial resolution.

The differences between the equivalent number of looks obtainable for a LR image derived from SLC, PRI and UI16 products in figures 2.1 to 2.3 are a clear demonstration that the quality of the LR imagery is dependent on the HR image type used to generate it. Even if the same bandwidth is used in the generation of two HR images (960 Hz for UI16 and PRI), the spatial resolution obtained for the UI16 image is poorer than the one obtained with the more thorough processing

8

performed to generate the PRI image. The SLC product uses a larger bandwidth (about 1400 Hz) which results in a significantly better radiometric resolution in the resulting LR image.

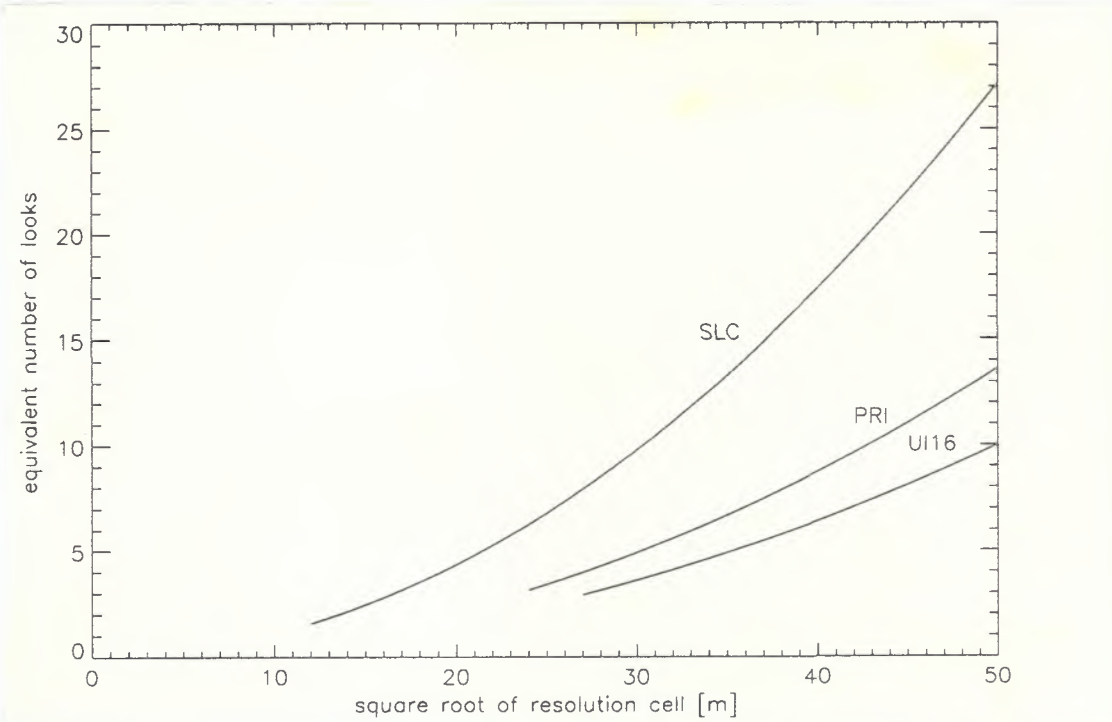

Figure 2.1 *Maximum obtainable Equivalent Number of Looks for SLC, PRI and UI16 derived Low Resolution imagery (0 to 50m)*

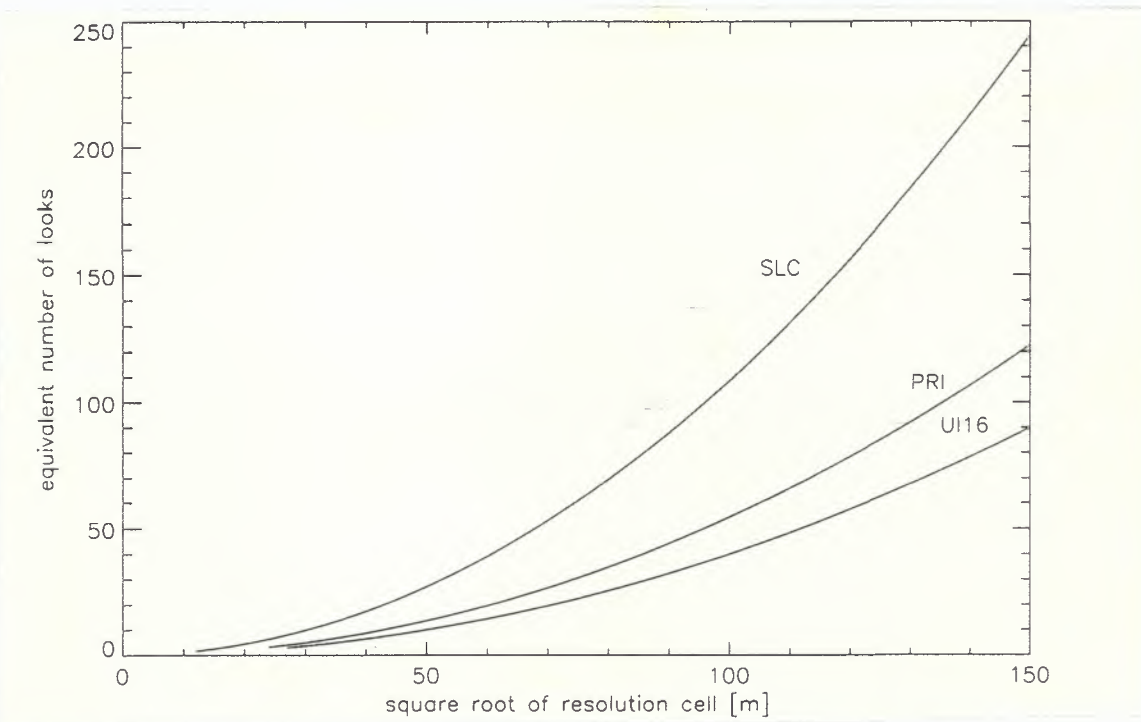

Figure 2.2 *Maximum obtainable Equivalent Number of Looks for SLC, PRI and UI16 derived Low Resolution imagery (0 to 150m)*

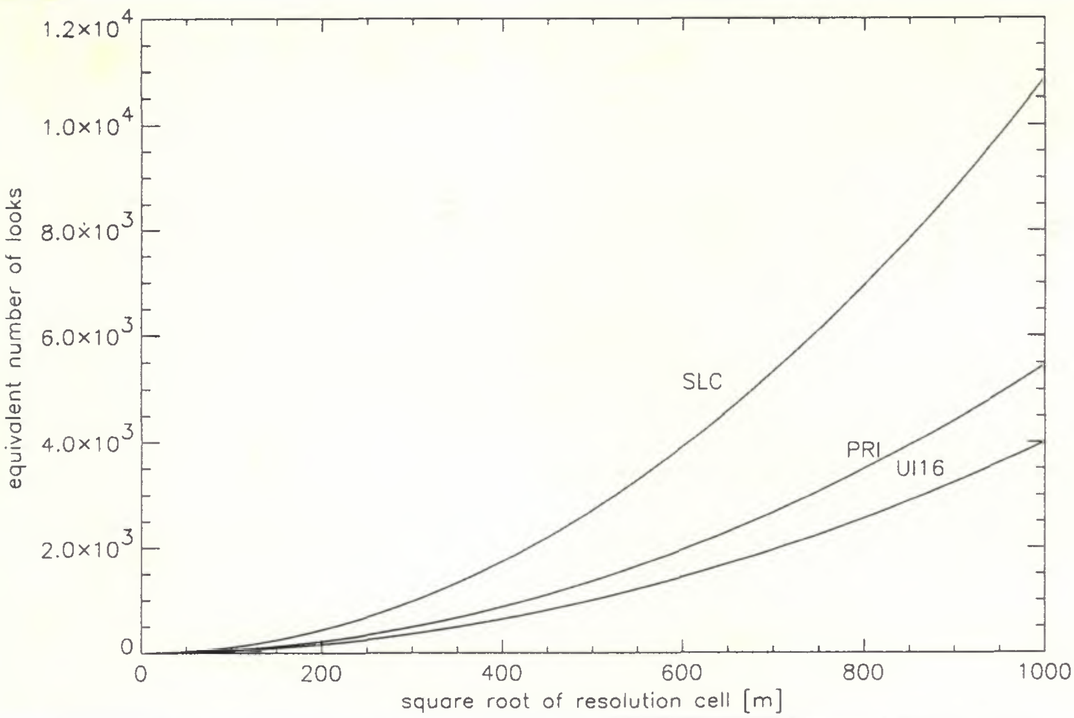

Figure 2.3 Maximum obtainable Equivalent Number of Looks for SLC, PRI and UI16 derived Low Resolution imagery (0 to 1000m)

2.1.2 Speckle reduction against processing time

In order to generate LR imagery with less computation power, one can choose to use only a part of the whole information contents (bandwidth) of the raw data by subsampling techniques. This implies that the speckle reduction will be poorer, but near real-time processing can be realized with use of limited computing resources. So-called "quick-look" products are based on such an approach (see chapter 4). The poor reduction of speckle limits the possible use of the digital product generated, but the reduced processing load enables image generation for all acquired raw data.

It should be underlined that the generation of HR products demands high computing power that significantly limit the access to the acquired raw data. Up to now more than 85 % of the acquired SAR data at the ESA ground stations are not processed.

2.1.3 Product size against dynamic range

This is mostly a question of 8 or 16 bit format on the amplitude version of the image, and is of issue because of the factor two reduction of data volume. The trade-off here is dynamic range against radiometric precision.
Here the issues are sufficiently clear that an optimal solution can be found which covers the needs of most applications. Experience has shown that most often this can be achieved with only minor loss of information (see section 2.3.2).

2.2 Image Processing Techniques for LR Imagery

In the following section, we review the different processing techniques used for LR imagery generation. Some of these techniques are used for the direct generation of the existing LR imagery (e.g. block averaging, pre-filtering of raw data) or for preparation of HR image before LR imagery generation (e.g. moving window averaging). Others (e.g. complex integration, complex block averaging) are used in our simulation of different radiometric resolutions in LR images (see chapter 5).

Block averaging (sum of N pixels divided by N):

Block averaging is the most straightforward technique in generation of LR imagery from HR detected products. Its goal is to reduce the data volume of the HR product while ensuring that all HR original pixels are represented in the resulting LR image. This is done by averaging neighboring pixels contained in a non-moving block (see figure 2.4).

The size of the resulting LR image is given by:

LR image size = HR image size / X . Y where X = Block size in X direction

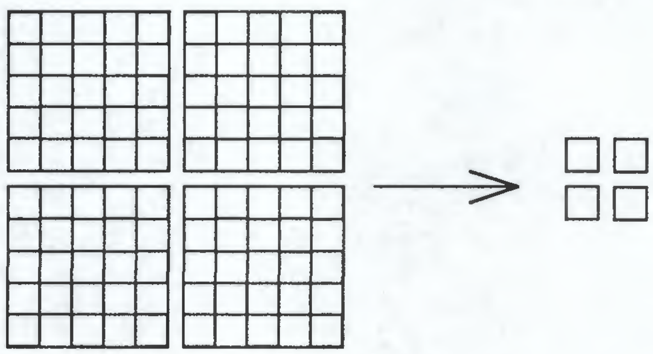

Figure 2.4 *The block averaging reduces the image size by averaging the pixels contained in the block area into a new pixel in the new image. For illustrations purposes the four non-overlapping blocks that generate the four new pixels have been separated by a small spacing.*

Before to discuss the outcomes of the block averaging techniques, it is important to remember that in theory a SAR detected image should satisfy the Nyquist criterium, i.e. that a SAR image shall be sampled at least twice the highest frequency (see Annex). This consideration is relevant only when the goal for LR generation is a LR digital product, not for LR display purpose.

11

The block averaging method produces an undersampled LR image. This results in poor correlation between neighboring LR pixels, specially when the natural correlation of the scene is low, i.e. where the speckle is fully developed (homogeneous areas). ***Poor correlation results in poor radiometric resolution*** (see section 3.1.2). Undersampling of the image results in aliasing. This is a real problem only when the resulting LR image has to be interpolated because in such a case the amount of spurious frequencies becomes excessive. ***Interpolation of LR images is necessary to generate geocoded LR images.***

Moving window averaging (low-pass filter):

This operation correlates detected data via convolution with a two dimensional kernel. This is equivalent to a low-pass filter.

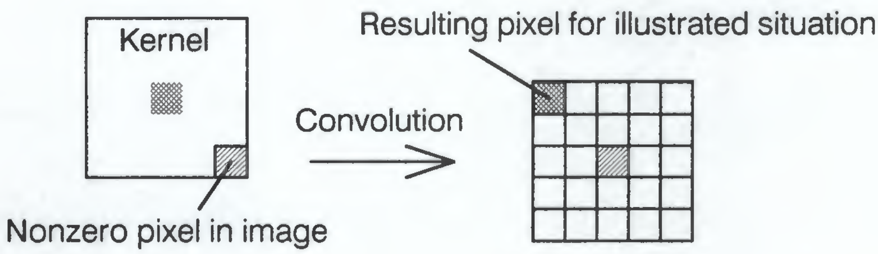

Figure 2.5 *The drawing illustrates the process of moving window averaging of a kernel (5 by 5 flat window) over an image. The impulse response is equal to the kernel.*

Figure 2.5 illustrates that a single pixel in the original image influences the value of many neighboring pixels in the output image when moving window average is applied. As the kernel sweeps over the image it repeatedly encounters one specific pixel in the original image, but at different offsets w.r.t. kernel centre.

To simulate various radiometric resolutions (see chapter 5) we use a flat kernel with all elements equal to 1. It is also possible to use weighted averaging e.g. triangular shape. The first method broadens the impulse response while the latter has a smoothing effect. The first method results in a higher equivalent number of looks in the image, linearly dependent on the number of independent image samples in the kernel area. The number of looks is given by NL x IS, where NL is the number of looks in original image and IS the number of independent image samples in the kernel area.

The moving window averaging technique should be applied before the block averaging in the generation of LR imagery from HR imagery.

Combination of Moving Window Averaging and Block Averaging:

A simple method to limit the amount of spurious frequencies generated by the block averaging technique is to apply first a low-pass filter (i.e. to perform a moving window averaging) on the HR image. The overall result is equivalent to a block averaging using a kernel which consists of a pyramidal cone as illustrated in figure 2.6 and 2.7.

Such a combination (first moving window averaging then block averaging) correlates adjacent pixels in the new image. The amount of correlation depends on the relationship between the kernel sizes. With odd numbers and equal kernel sizes (as with figure 2.4 and 2.5) the neighboring pixels in the final image will together have contributions from all but the central pixel.

Complex integration (moving window averaging on complex data):

This technique transforms a complex image without changing its size. A complex summation (i.e. mean of I and mean of Q channel) is performed over a window around each sample to generate its new value. This is performed by moving the window (by step of one sample) over the entire image.
Where speckle is fully developed (without dominant scatterers in the resolution cells) the result of such an operation is expected to be zero, but it will in most real situations result in a small non-zero value. When the phase is coherent, as it is in the presence of a dominant scatterer in the resolution cell, the result of this operation gives the integrated energy returned from this scatterer [Ref. 2, 3]. This operation broadens the area of influence of the strong scatterers and integrates the full energy of the object. This ensures that the energy of point targets is preserved in the output image. About half of the dynamic range of the data is reduced during this operation.

1	2	3	4	5	4	3	2	1
2	4	6	8	10	8	6	4	2
3	6	9	12	15	12	9	6	3
4	8	12	16	20	16	12	8	4
5	10	15	20	25	20	15	10	5
4	8	12	16	20	16	12	8	4
3	6	9	12	15	12	9	6	3
2	4	6	8	10	8	6	4	2
1	2	3	4	5	4	3	2	1

Figure 2.6 *Example of a kernel resulting from a moving window averaging followed by a block averaging (5 x 5 kernel sizes for both averaging).*

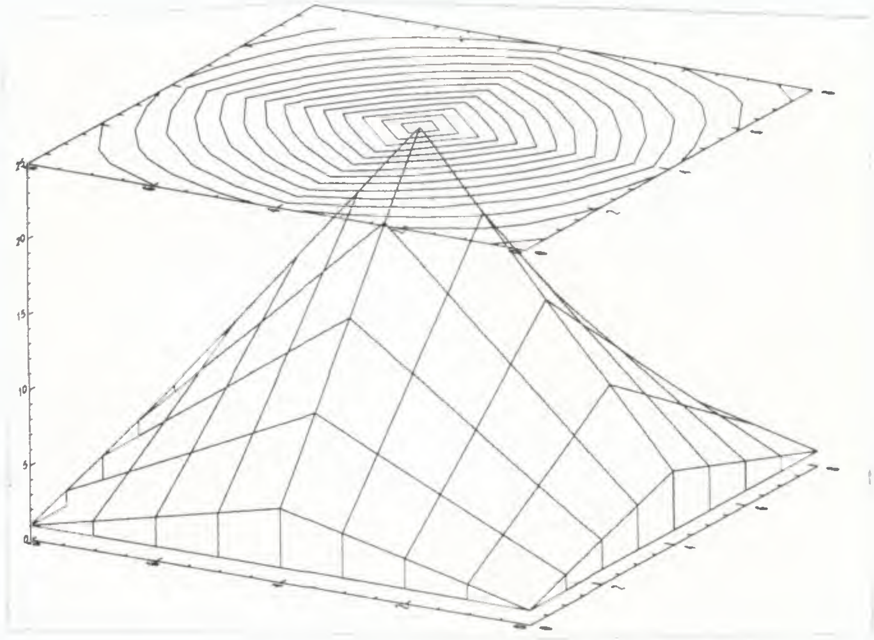

Figure 2.7 *The total kernel from fig. 2.6 in graphic representation. It can be described as a pyramidal cone.*

Complex block averaging (fixed window averaging on complex data):

This technique transforms a complex image by changing its size. As previously, a complex summation is performed over a window around each sample to generate its new value. But the window is fixed (block-averaging technique). This operation reduces the spatial sampling rate of the original image and thereby reduces the information content of the LR image.
With this technique, we can simulate different radiometric resolutions in LR images while keeping constant spatial resolution. The dynamic range is slightly reduced by this operation.

Integer subsampling:

The image size is reduced by extraction of each Xth column and each Yth row, where X and Y are integers. The rest of the data is discarded without influencing the new image.

Pre-filtering of raw data:

Raw data pre-filtering is one of the most straightforward technique used in generation of LR imagery derived from raw data. Its goal is to reduce the raw data volume before processing (e.g. pre-summation or sub-sampling) in order to save computing power. Raw data volume reduction means information content (or equivalently bandwidth) reduction. This degrades the final product by poorer speckle reduction for a given spatial resolution and vice-versa. The resulting loss of information is illustrated in the simulation in chapter 4.

2.3 16 TO 8 BIT CONVERSION

As discussed in section 2.1 a data volume reduction by a factor two is possible with a 16 to 8 bit conversion of the amplitude LR image. This should be done only if it can be achieved with a minimum loss of information.

The dynamic range of backscattering coefficients σ^o in C-band, VV polarization and 23 degrees of incidence angle is ***within 35 dB*** (ranging from -30 dB to 5 dB) for natural targets (ocean, ice, vegetation, terrain). Since 8 bits representation gives a σ^o dynamic range of 48.1 dB, it is feasible to store ERS SAR data in 8 bits without significant loss of dynamic range for most distributed targets.

Manmade objects, specially in built-up areas, have radar cross sections σ higher than 5 dB. But radar cross sections analysis is an HR imagery activity. In LR imagery the interest is exclusively on large distributed targets, i.e. on backscattering coefficients σ^o.

When the goal for LR imagery generation is ***display*** (browse function), the converted LR image must appear as contrasted as possible, i.e. with a good visual quality. The contrast enhancement can be obtained using histogram equalization (available in all image processing softwares). An additional data compression can be obtained with various compression algorithms [Ref. 4].

When the goal for LR imagery generation is a ***LR digital product***, two criteria must be fulfilled by the conversion:

1. it shall be linear to preserve the original radiometric information,
2. it shall be possible to calibrate LR digital products after conversion.

Both these criteria rule out the use of histogram equalization since this irreversibly changes the probability distribution in the image and thereby changes the radiometric information. Any radiometric comparison between histogram-equalised LR images becomes speculative and of questionable scientific and applications use.

Two possible techniques for 16 to 8 bit conversion are presented herein. The first one is a flexible conversion technique which fits to the HR image pixel distribution and which is suitable for LR display purpose. The second one is a fixed conversion technique which is suitable for generation of LR digital products.
Techniques involving hybrid conversions (e.g. multilinear, square root, logarithmic conversions) are not addressed here.

2.3.1 Distribution Dependent Conversion

A distribution-dependent conversion can be achieved using either the probability density function or using the first order statistics (mean and standard deviation) of the original pixel values.

The conversion using the probability density function of the original HR image is usually done via two steps:

1. histogram equalization
2. linear conversion

16

Histogram equalization redistributes the pixel values so that there are approximately the same number of pixels with each value. The result is a nearly flat histogram. The consequence is an image contrast enhancement.
The linear conversion is done via a division of the pixel values (division by 255 for conversion from 16 bits to 8 bits).
The histogram equalization method can be combined or substituted with a histogram matching (to Gauss distribution or Gamma distribution).

Instead of using a conversion based on the histogram, one can use the statistics (mean and 3 standard deviations) of the original image to choose the portion of the HR image where to apply the linear conversion. The mean and standard deviation are available in the annotations of ESA ERS products (PRI, UI16). However the results obtained with this method are not as good as the histogram equalization for contrast enhancement.

The distribution-dependent conversion destroys the original radiometry. However laborious methods can be used to reverse the conversion process if it has been documented in the LR product headers [Ref. 5].

2.3.2 Fixed Linear Conversion

This method uses a fixed linear conversion of the portion of the original image containing the radiometric information. The conversion factor is a constant ratio R. This implies that qualitative and quantitative comparisons between resulting LR images can be done without further processing.

$$DN_{new} = DN_{old} / R \qquad \text{where } DN = \text{pixel value}$$

$$\text{If } DN_{new} > 255, \text{ then } DN_{new} = 255$$

The choice of the constant ratio R is dependent on the original HR image radiometry. An example of derivation of constant ratio factor is given in section 3.1.1.

One advantage of this method is the possibility to have absolutely calibrated LR products. If the original HR product has a calibration constant K, then the calibration constant of the resulting LR image is K/R. Calibration corrections like antenna pattern compensation can be applied either on the original HR product, either on the resulting LR product.

3 LR IMAGERY DERIVED FROM HR PRODUCTS

In this chapter we review existing ERS-1 LR imagery derived from High Resolution products.

3.1 UILR PRODUCT

The UILR product is created by ESA/ESTEC [Ref. 5] and derived from the ESA Fast Delivery HR product called UI16 [Ref. 1]. The UILR product happens to be available in digital form. It has been developed mainly to serve real-time applications in the field of sea ice monitoring. ***It means that the UILR product is primarily intended to serve as a display (or browse) of UI16 product, not as a LR digital product as such.***

However three improvements would be sufficient to consider the UILR as a 'true' digital LR product. Our proposal for improvements on the UILR product specifications concerns the following problems. Firstly we address the effects of the ***histogram equalization technique*** on the original radiometry. We then explain that the UILR ***radiometric resolution*** can be improved if low pass filtering is applied on UI16 product before the spatial reduction by block averaging. Finally we comment the method used to obtain a 6.3 ***reduction rate in azimuth.***

3.1.1 Conversion 16 to 8 bit

This is the main area in which the UILR product can be improved.

The UILR product was created for a specific use: to serve real-time applications in ice monitoring, i.e. for display purposes only. However the UILR product is now considered as a true digital product by a majority of users. As explained in section 2.3, it is difficult to propose LR imagery satisfying at the same time display purposes and digital product purposes.

The original 16 bit dynamic range of the UI16 image (in fact 15 bits) is mapped into an 8 bit representation by use of a histogram equalization method. This is done to allow an immediate visual representation of the image (display purpose), but destroys the radiometry and makes qualitative and quantitative comparisons between UILR products troublesome (inverse process by use of the annotations and a look-up table).

A possible method to reverse the conversion process is proposed in the UILR specifications [Ref. 5]. However the reverse process is laborious to perform and

results in an unstable radiometric precision. Local distributions located in the lower or the higher end of the total distribution (e.g. bright ice fields or smooth water surfaces) can be contained within only a few intensity levels. In such a case estimation of the local mean and standard deviation values may be disturbed. Then local statistical properties of images are not the same and cannot be used for classification.

The ***proposed solution*** in order to considered UILR product as a true digital product is to perform a fixed conversion by dividing the pixel value in the UI16 image by a constant ratio factor R (see section 2.3).

To define the conversion constant R, we analysed the headers of more than 15000 UI16 products produced at Kiruna and Fucino ground stations between August 1991 and December 1992. Given the acquisition stations, the analysed UI16 products cover a fully representative type of surfaces (ocean, sea ice, glaciers, vegetation, desert and built-up areas). Such an analysis is valid only if the processor gains have never been changed, which is the case for the FDP processors since the beginning of the ERS-1 mission.

We found that the mean of the UI16 pixel values lies between the extreme values of 250 and 4000, with an average mean of 1700. Converted in decibels, it gives a mean dynamic range of 24 dB in agreement with what was expected and well within the 48.1 dB available in an 8 bit product. It should be noted that previous values (250 and 4000) are extreme values and that most of mean values are within a range 700 - 3000 (see figure 2.8).
As expected (speckle distribution in 3 non-overlapping looks image), the standard deviation is strongly correlated to the mean (ratio of st. dev. / mean equal or superior to 0.294), which means that high standard deviation shall be expected in high mean images (see figure 2.8).
We also found that the monthly average mean is relatively constant along the analysed period : it varies from 1600 to 1800, i.e. 1 dB of variation.

Given the previous results (UI16 mean value = 1700), the proposed ratio number is ***R** = 20*. This number leads to a mean average value equal to 85 (1700 / 20) in UILR products. This is compatible with the shape of the original Gamma distribution (more extreme values in upper end). The 'bright' images will have a mean value about 150 while the 'dark' image will have a mean value about 30.

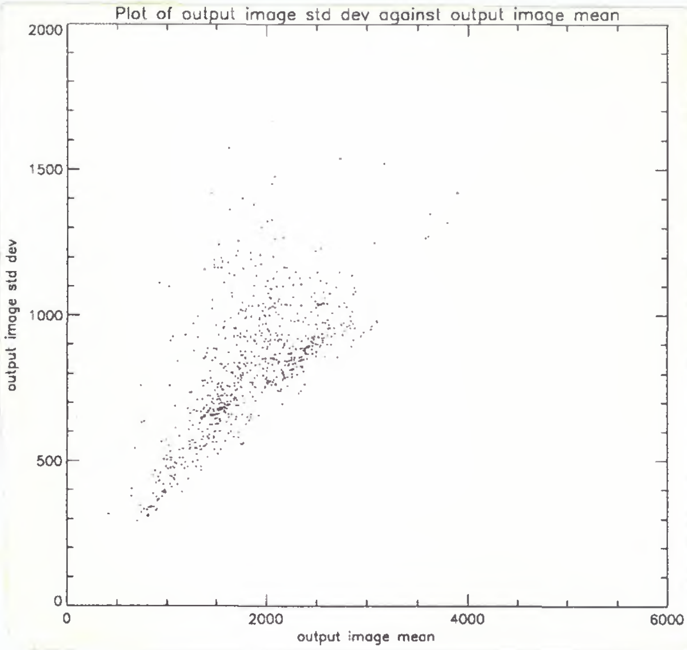

Figure 2.8 UI16 mean plotted against UI16 standard deviation for December 1992.

3.1.2 Non optimal radiometric resolution

The UILR product is created with the block averaging technique (see section 2.2). When only block averaging is applied, the resulting information changes too rapidly from pixel to pixel. One has introduced spurious frequencies. The main consequence for a LR image is a reduced radiometric resolution. Another consequence is the distortions in pixel intensities if resampling is performed on the resulting image (as it is the case for UILR).

On the contrary if low-pass filtering is applied to the original image (see section 2.2), the amount of spurious frequencies is reduced (depending on the filtering kernel size and on the weighting function), the radiometric resolution is greatly improved and resampling can be applied without severe side effects.

In order to demonstrate the poor radiometric resolution resulting from a simple block averaging, we generated an improved UILR (image 2) with a moving window averaging followed by a block averaging and we compared it to the corresponding standard UILR (image 1).

The kernel sizes are chosen to limit the amount of spurious frequencies introduced by the block averaging (by increasing the correlation between neighboring pixels in the output image), while keeping similar data volume (and reasonable processing time). The kernel sizes used to generate the improved UILR are the following :

	Moving Window Averaging	Block Averaging
Range	6	5
Azimuth	9	6

Other types of kernels could be used (i.e. bell shaped) at a cost of computational load.

The following tables give the results of the quality measurements done on the standard UILR and improved UILR. The IRF measurements (spatial resolution and PSLR) are obtained with a point target of opportunity found in the image.

Standard UILR (image 1)

Range pixel spacing	:	100 m	Azimuth pixel spacing (non fixed)	:	95.4 or 111.3 m
Measured range resolution	:	1.41 pixels = 141 m	Measured azimuth resolution	:	1.26 pixels ≅ 130 m
Measured PSLR	:	12 dB	Measured E.N.L.	:	*32*

E.N.L. = Equivalent Number of Looks

Improved UILR (image 2)

Range pixel spacing	:	100 m	Azimuth pixel spacing (fixed)	:	95.2 m
Measured range resolution	:	1.50 pixels = 150 m	Measured azimuth resolution	:	1.55 pixels ≅ 148 m
Measured PSLR	:	12 dB	Measured E.N.L.	:	*70*

Compared to the standard UILR, the improved UILR has a very good radiometric resolution (about 40 additional equivalent looks) and a slightly better spatial resolution (with respect to the Nyquist criterion).

The improvement in radiometric resolution is due to the low-pass filtering process that correlates the scene where the scene itself is not coherent. The slight improvement in resolution cell size is due to the low-pass filtering kernel size too small to influence the natural correlation of strong scatterers.

The pixel spacing is fixed with a 5% difference between range and azimuth directions. It means that a further resampling (in order to obtain square pixel spacing) can be performed with less distortion than on the standard UILR.

Image 1 : UILR. The scene shows the Ems estuary at the border between Germany and the Netherlands. The German town of Emden lies north-east of the river outlet, while parts of the Dutch town of Groningen are seen in the south-western corner of the image. In the north-western corner one can see some of the East-Frisian islands.

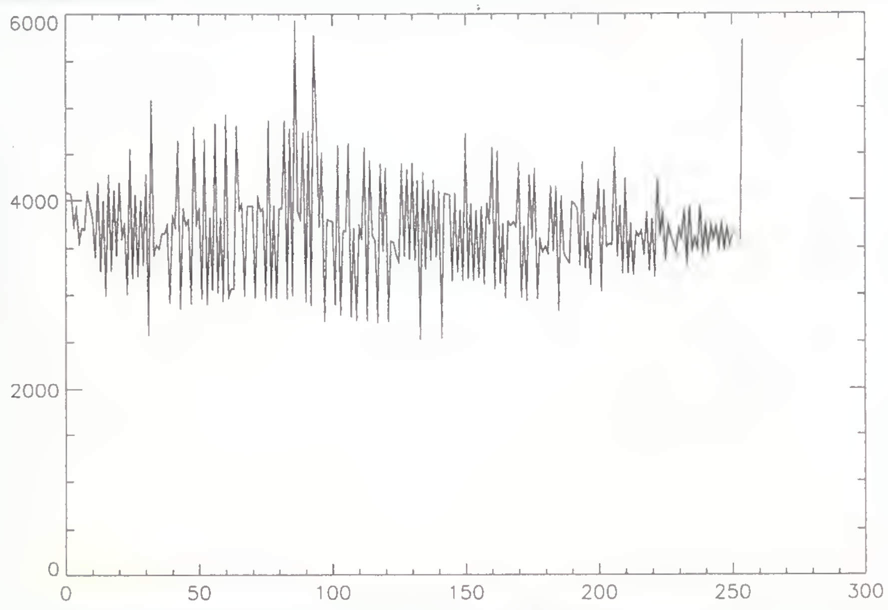

Figure 3.1 Histogram of Image 1

82

Image 2 : UI16 to 'UILR' before histogram equalization, but with better sampling introduced by low-pass filtering. The image has been transformed to 8 bit and restored to intensity before printing.

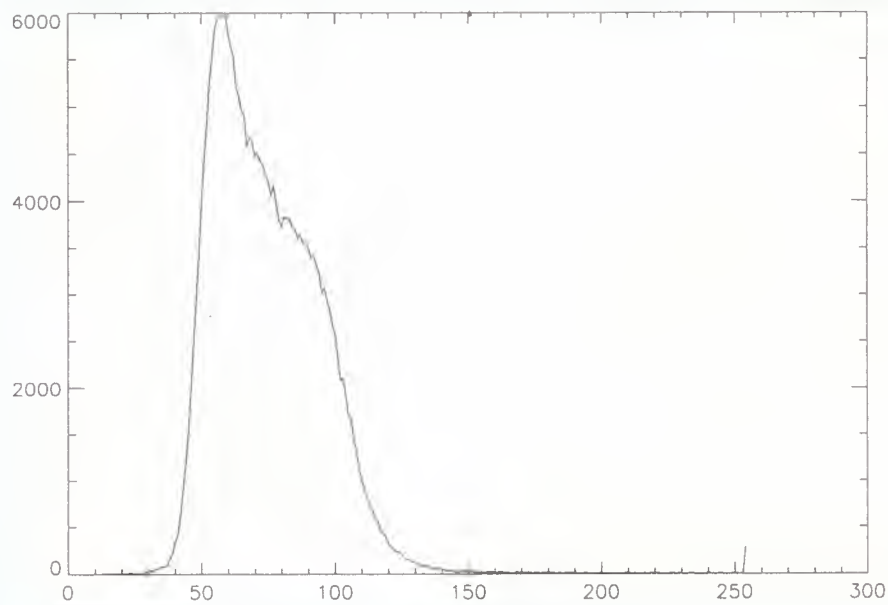

Figure 3.2 Histogram of Image 2, 8 bits

3.1.3 Reduction rate in azimuth

To obtain an image with 1000 by 1000 output pixels from the original UI16 containing 5000 by 6300 pixels, an alternating block averaging kernel size is used. This means that two kernel sizes are used: a 5 by 6 kernel (generating 700 lines with azimuth pixel size of 95.4 m and geometric distortion of 4.6 m) and a 5 by 7 kernel (generating 300 lines with azimuth pixel size of 111.3 m and geometric distortion of 11.3 m). About each third line is then generated by the largest kernel, and therefore covers a larger area than the two preceding lines. Alternation between these two kernels produce local distortions at the scale of 15.9 m.

By using only one kernel size (5 by 6) in the block averaging process, one generates a fixed geometric distortion of (5 x 20) - (6 x 15.9) = 4.6 m. The size of the resulting product (see previous section) is 1000 x 1050 pixels. The fixed geometric distortion can then be corrected by users with a resampling method, while the correction of the alternating 15.9m local distortion is more difficult.

3.2 TROMSØ LRI PRODUCT (TSS)

The LRI (Low Resolution Image) product is a LR digital product produced by the Tromsø Satellite Station (TSS) and derived from the TSS HR product called FRI (Full Resolution Image). The FRI product specifications [Ref. 6] are similar to the ESA FD product specifications (UI16), i.e. 3 looks, same pixel spacing, no calibration correction.

The main advantage of the LRI product is its production throughput superior to the UILR production throughput. The generation time (including the processing time of the full resolution image FRI) is 8 minutes. Up to now, about 15 LRI products per day are generated. This is however far from the LR processing of all raw data acquired by the ground station.

The LRI product is obtained via a 5 x 5 averaging of the FRI product. We understand from Ref. 6 that this is a simple block averaging, which results in non optimal radiometric resolution and undersampling of the LRI product (see section 3.1.2). Given the spatial resolution of the FRI product : 22.5 x 26 = 585 m^2 (slightly better than the spatial resolution of the UI16 product : 25 x 28 = 700 m^2) and the 5 x 5 block averaging (instead of 5 x 6 for UILR), we estimate the equivalent number of looks to be the same than for the UILR, i.e. about 30.

The LRI product size is 1000 by 1260 pixels which results in a pixel spacing of 100m in ground range and 80m in azimuth. Resampling by interpolation of the LRI product to obtain a square pixel image will introduce uncertainties in statistical analysis of the resulting product due to the undersampling present in the LRI.

As proposed in the previous section, a low filtering of the FRI product would increase the radiometric resolution and allow further resampling of the image.

The 16 bit representation is preserved in the final image. This maintains the dynamic range, and leaves the users to decide about an eventual reduction of the data volume.

3.3 GATINEAU SGC PRODUCT (CCRS)

The SGC (SAR Georeferenced Coarse-Resolution) product is an ERS LR digital product produced by the Canada Centre for Remote Sensing (CCRS) at the Gatineau ground station and derived from the Canadian ERS HR product called SGF (SAR Georeferenced Fine-Resolution). The main SGF product specifications [Ref. 7] are the followings: 6 looks , 16-bit pixel, 12.5 m x 12.5 m pixel spacing, no calibration correction.

The SGC product is generated by 4 x 4 averaging the SGF product [Ref. 7]. As for the previous products, this results in an undersampled product. However, since the HR SGF product has uniform pixel spacing in range and azimuth, it is unlikely that the SGF product will be resampled.

The SGC product size is 2000 by 2000 pixels which results in a pixel spacing of 50 m by 50 m. We understand from the product specifications that the pixel is either coded on 16 bits or 8 bits. No information is available on the conversion method from 16 to 8 bits.

3.4 FAIRBANKS LOW RESOLUTION PRODUCT (ASF)

The Fairbanks ERS Low Resolution product is a LR digital product produced by the Alaska Station Facility (ASF) and derived from the ASF ERS Full Resolution product whose specifications [Ref. 8] are the followings: 4 looks, 16-bit pixel, 12.5 m x 12.5 m pixel spacing, calibration correction.

The Lo. Res. product is generated by 8 x 8 averaging the Full Res. product [Ref. 8]. This can be interpreted to be a block averaging resulting in undersampling. However this undersampling is acceptable since, the HR product having square pixel size, there is no need to resample the Lo. Res. product.

The Lo. Res. product size is 1000 by 1000 pixels which results in a pixel spacing of 100 m by 100 m. The pixel is coded on 8 bits.

The main advantage of the ASF Lo. Res. product is its high throughput rate due to the short processing time of the Full Res. product (about $1/24^{th}$ real time). At the end of 1992, about 50 % of the ASF acquired raw data was processed at Full Resolution and by consequence at Low Resolution.

ASF proposes another LR product : the Geocoded Lo. Res. product derived from the Geocoded Full Res. product using the method described previously.

4 LR IMAGERY DIRECTLY DERIVED FROM RAW DATA

Such imagery is derived from the raw data without to first process at full resolution. Its advantage is the ability to completely cover the acquisitions made by the SAR instrument and by consequence to assist users in the choice of high resolution production requests.

Its disadvantage (up to now) is the poor radiometric resolution of the obtained products. It means that such an imagery cannot be used as a digital products for the time being.

In this chapter we do a review of the existing LR imagery (often called real time image or quick look image) obtained by such a technique.

4.1 BRAZIL QUICK LOOK (MDA)

The Brazil ERS SAR quick look is generated at the Cuiaba ground station (INPE) by a processor designed and built by MDA.
In the available documentation [Ref. 9] the data synthesis is not described. However the main processing parameters are given : the image is presented in slant-range (8 bits per pixel) with pixel spacing of approximately 25 m in slant range (about 64 m in ground range) and approximately 85 m in azimuth. The spatial resolutions are quoted : in slant range less than or equal to 47m, in azimuth less than or equal to 120 m (at mid-range) but varying across track (158m at far range).
The number of looks is 12.

4.2 GERMAN ANTARCTIC QUICK LOOK (DORNIER)

The Antarctica ERS SAR quick look is generated at the O'Higgins ground station (operated by DLR) with a processor designed and built by Dornier.

The Dornier processor is a "true" real time processor able to deliver low resolution image with the following parameters [Ref. 10] : slant or ground range image of 80 km of the swath width, pixel spacing about 90 m in ground range by 90 m in azimuth, spatial resolution about 100 m in both directions, pixel coded on 16 bits.

The range compression is performed in frequency domain. In azimuth, 16 azimuth looks are generated with the Spectral Analysis (SPECAN) algorithm. The equivalent number of looks has not been measured.

4.3 MBB QUICK LOOK

This quick look processor has been developed by MBB [Ref. 11]. This is a real-time SAR processor based on transputer technology.
The quick look image is generated by subsampling in the azimuth direction after a frequency shift and two times convolution by an unweighted kernel. That is equivalent to pass-band filtering the frequency spectra with a triangle function. The process can be tuned to produce the desired range spatial resolution. After this operation look summation is performed in range. This implies that the equivalent number of looks is between 4 and 6 for spatial resolutions in the range 90m to 140m.

4.4 BANGKOK QUICK LOOK (MATRA/ACS)

The Bangkok ERS SAR quick look will be generated at the Bangkok ground station (NRCT) by a processor under development at Matra MCS and ACS and with an algorithm proposed by Politecnico of Milan [Ref. 12]. The system will be operational early 1994.

The processing scheme adopted uses data reduction techniques both in range and azimuth. Low-pass filtering and subsampling by a factor of 2 in range and by a factor of 4 in azimuth is performed on the raw data. This reduces the computational load for the image generation. Subsequently look extraction is performed both in range and azimuth; 2 looks in range and 4 looks in azimuth, resulting in eight slightly correlated looks.

Spatial resolutions of about 50 m in slant range (about 128 m in ground range) and 100 m in azimuth and 6.4 looks have been measured in the resulting products.

The processing time of the QL processor will be better than 1/8th real time.

Image 3 gives an example of Bangkok QL image.

Looking to future improvements in the quality of the Bangkok QL (i.e. increase in number of looks), we produced a low resolution product where four QL images with slightly correlated speckle are generated and summed. This results in a LR image (image 4) with about 24 looks and the same spatial resolution as the individual quick-look images. This was done by superposing and averaging pixel by pixel four images where different band-pass filters in the azimuth data reduction technique have been used.

By applying a band pass filter to extract the complementary information from the raw data in the range filtering process one can obtain another four low resolution images to produce a total of eight slightly correlated 6.4 look images. This would result in a LR image with about 45 equivalent looks, i.e. a LR digital product suitable for scientific applications. By eightfold parallel processing this product could be available in near real-time.

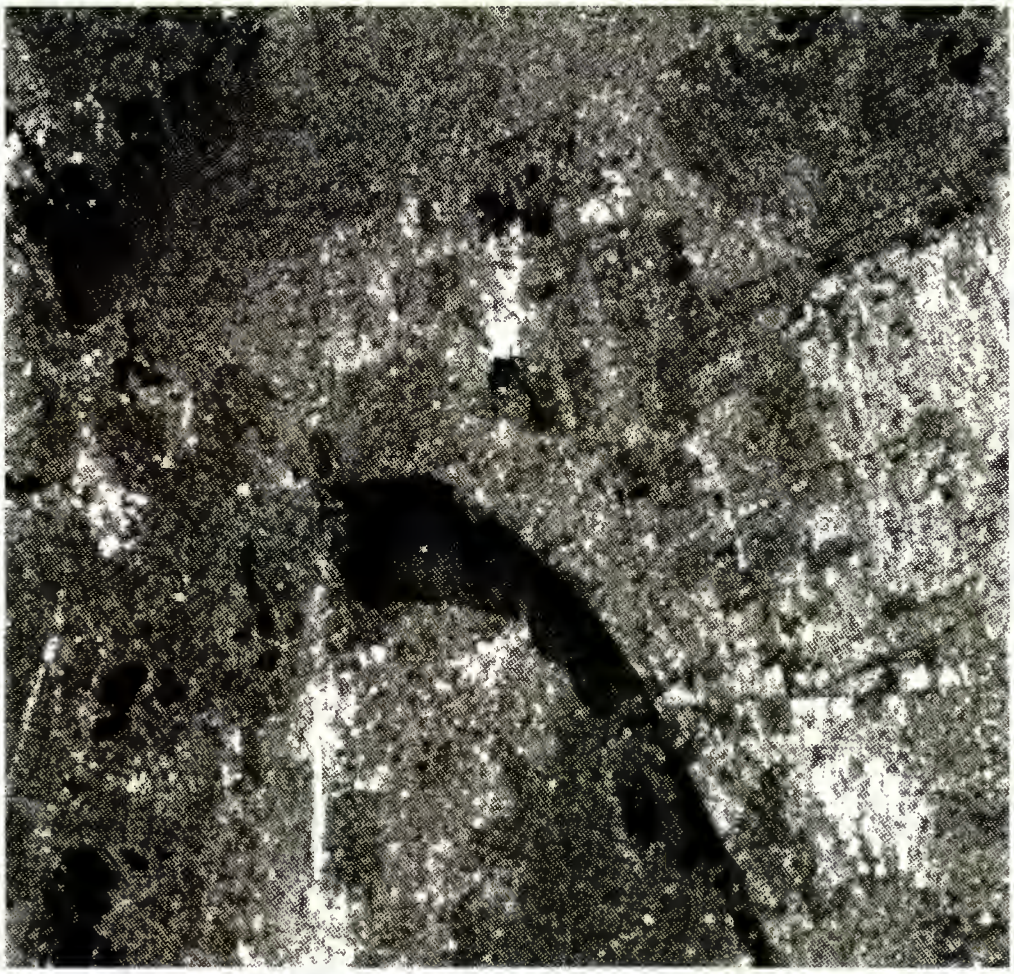

Image 3 *Example of Bangkok Station Quick Look image (6.5 eq. nb. of looks), 19 September 1991, intensity (see description of the area in section 5.1.1)*

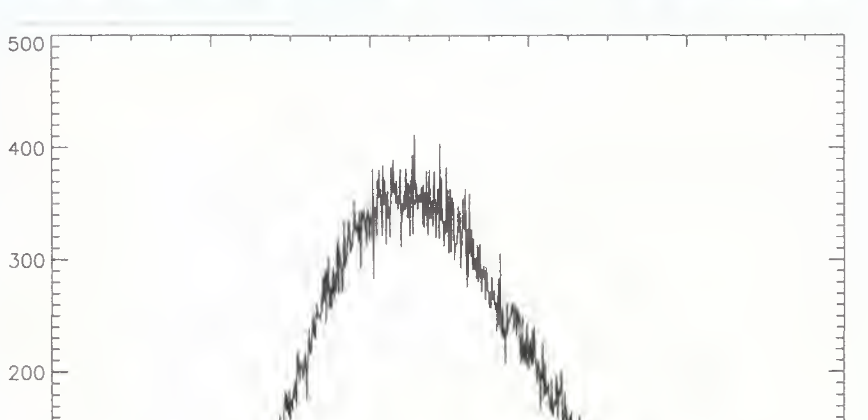

Figure 4.1 *Histogram of Image 3.*

30

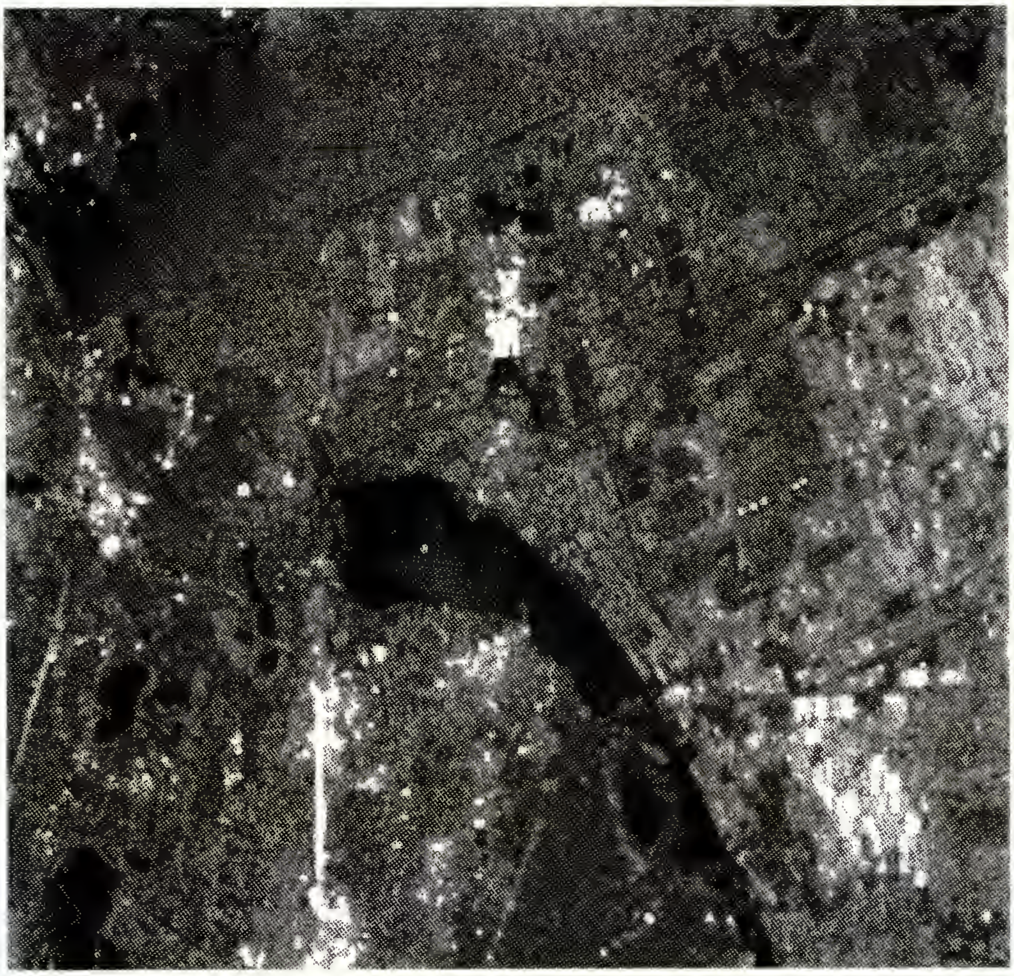

Image 4 *Example of quality improvement of QL image (same scene than image 3) : 24 eq. nb. of looks.*

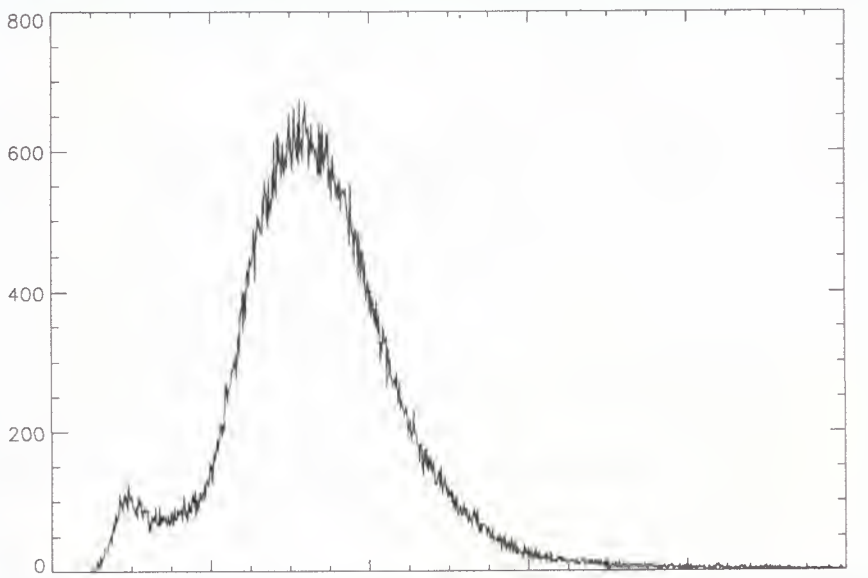

Figure 4.2 *Histogram of Image 4*

5 SIMULATION OF DIFFERENT RADIOMETRIC RESOLUTIONS IN LR IMAGERY

The purpose of the simulation is to visually demonstrate the effect of speckle noise reduction in low resolution SAR products. This is useful for the comparison between specifications and can also be of interest in defining minimum criteria to be applied in future developments.

Although the radiometric resolution is the main image quality parameter in LR imagery, the differences between QL image (image 3) and simulated LR image (image 5) clearly demonstrate that other parameters contribute to the quality of a LR image. Both images (acquired at 9 days interval) have about the same spatial and radiometric resolutions, but the simulated image (image 5) shows distinct textural and radiometric differences from the Bangkok quick-look image (image 3).

In the chapter we first simulate LR image starting from HR complex data with 100 m spatial resolution and with different levels of radiometric resolution. We then do the same exercise starting from HR detected data. Finally we do an exercise of simulation of LR images with 1 km spatial resolution.

5.1 HR COMPLEX DATA TO 100 METRES RESOLUTION IMAGE

In the first part of our study, we simulate different levels of radiometric resolution (or equivalent number of looks) in LR images having spatial resolutions of about 100 m, i.e. pixel spacing about 50 m. Starting from HR complex data we can simulate varying radiometric resolutions with fixed spatial resolution by use of the complex block averaging technique (see section 2.2). We start from HR single look complex data but HR multilook complex data could also have been used.

5.1.1 Description of the Complex Data used in the Simulation

The HR complex data used in the simulation is a part of the product used by the ECISAR data quality group [Ref. 13, 14]. It is a slant range single look complex product processed with the VMP at ESRIN and having the following characteristics:

- Doppler bandwidth : 1332 Hz
- No windowing
- Sample spacing : 7.9 m in slant range, 4.0 m in azimuth

The image has been acquired on 10 September 1991 and covers part of the Flevoland region in the Netherlands.

The image is about 25 km x 32 km large and is described in figure 5.1. The region is flat and consists of forests and fields of different sizes, built-up areas and open water. Part of the city of Amsterdam can be seen on the top left of the image. In the bottom centre are the towns Bussum and Hilversum. The little town Almere-Stad can be found in the Flevoland polder almost at the centre of the image.

This image contains one of the ESA transponders used for the calibration of the SAR products, as well as several corner reflectors. The latter ones are difficult to visually detect since the backscattering level of the immediately surrounding terrain is relatively high. The transponder is located on the west of Almere-Stad. Details of manmade infrastructure such as sea walls, roads, railways and isolated habitations are clearly visible. To the north of the transponder a breakwater construction can be seen parallel to the land. The built-up areas and isolated constructions are the brightest features in the images. Forests are slightly brighter than suburban areas. The railways appear as bright lines and the roads (highways) as dark lines.

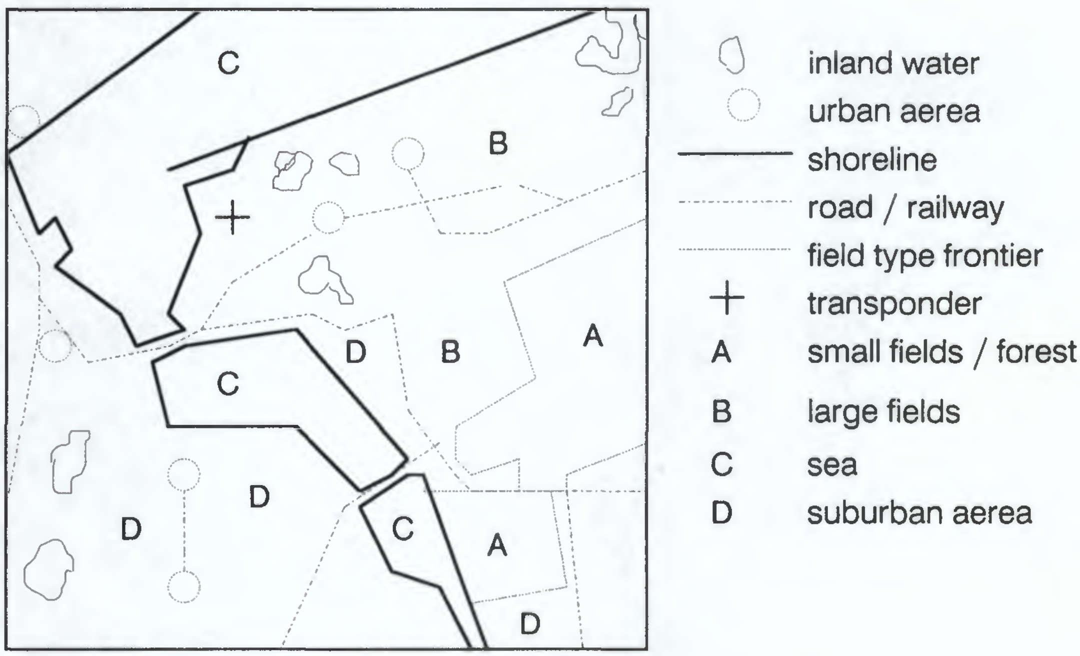

Figure 5.1 Description of the image used in the simulation.

5.1.2 The Method and the Results

The simulated images are generated using the following process (see section 2.2) :

Complex Integration → Complex Block Averaging → Detection → Moving Window Averaging → Block Averaging

Each simulated image is presented on the following way :

- Nominal number of looks
- Expected equivalent number of looks (resolution cell size of the detected image taken into account)
- Image number

The following table is used to summarize the different kernel sizes used in the processing :

	Comp. Integr.	Comp. B. Aver.	Moving W. Av.	Block Aver.
Range	A	C	E	G
Azimuth	B	D	F	H

- A and B give the kernel sizes in range and azimuth used in the complex integration performed on the HR image.
- C and D give the complex block averaging factors used to generate a smaller sized image prior to detection.
- E and F are the kernel sizes used for the moving window averaging on the detected image resulting from the complex processing.
- G and H are the block averaging factors in range and azimuth used to generate the final detected LR image.

When detected images are used as input for the simulation (see sections 5.2 and 5.3), cells A to D are left out.

For each simulated LR image, the following quality measurements are given :

- radiometric resolution, i.e. measured equivalent number of looks
- point target analysis, i.e. measured spatial resolution (3 dB widths) and PSLR

The quality analysis has been performed with the ESRIN SAR Quality Analysis System, "SARCALQ".

5.1.3 1 Look LR image (Image 5)

The HR complex data is averaged only prior to detection. There is no further processing of the detected data.

Simulation processing parameters :

	Comp. Integr.	Comp. B. Aver.	Moving W. Av.	Block Aver.
Range	3	3	1	1
Azimuth	13	13	1	1

LR image quality measurements :

Radiometric resolution :

Nominal Number of Looks :	1
Expected Equivalent Number of Looks :	1
Measured Equivalent Number of Looks :	***0.5***

Point target analysis :

Slant range pixel spac.	:	≅ 24 m	Azimuth pixel spacing	:	≅ 52 m
Measured ground range resolution	:	1.21 pixels ≅ 74 m	Measured azimuth resolution	:	1.23 pixels ≅ 64 m
Measured PSLR	:	10 dB			

The measured spatial resolution of the resulting LR image is largely under the Nyquist criterion. The change in spatial resolution in the complex image is negligible for the chosen kernel size (tested by applying only complex block averaging before detection).

The low equivalent number of looks can partly be explained by aliasing in the detected image due to the violation of the Nyquist sampling ratio.

As can be seen in image 5, the complex integration preserves and enhances strong scatterers in the resulting LR image.

The large standard deviation in the LR image makes interpretation very difficult. One can identify large structures such as the shorelines in the vicinity of calm water and some of the large built-up areas. It is also possible to identify some of the roads and railways as dark and bright linear features in the image.

A part of the breakwater structure north of the transponder has been plotted in three dimensions in figure 5.2. The breakwater structure itself has disappeared, only the calm water at the south of it can be seen as an unspeckled area. The land is difficult to distinguish from the sea.

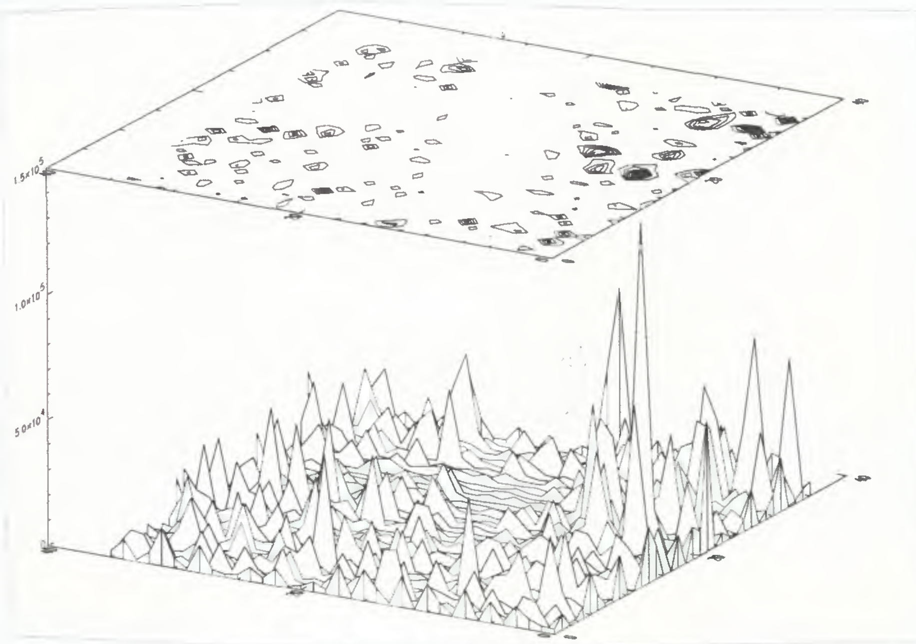

Figure 5.2 Three dimensional plot of breakwater structure for 1 look LR image.

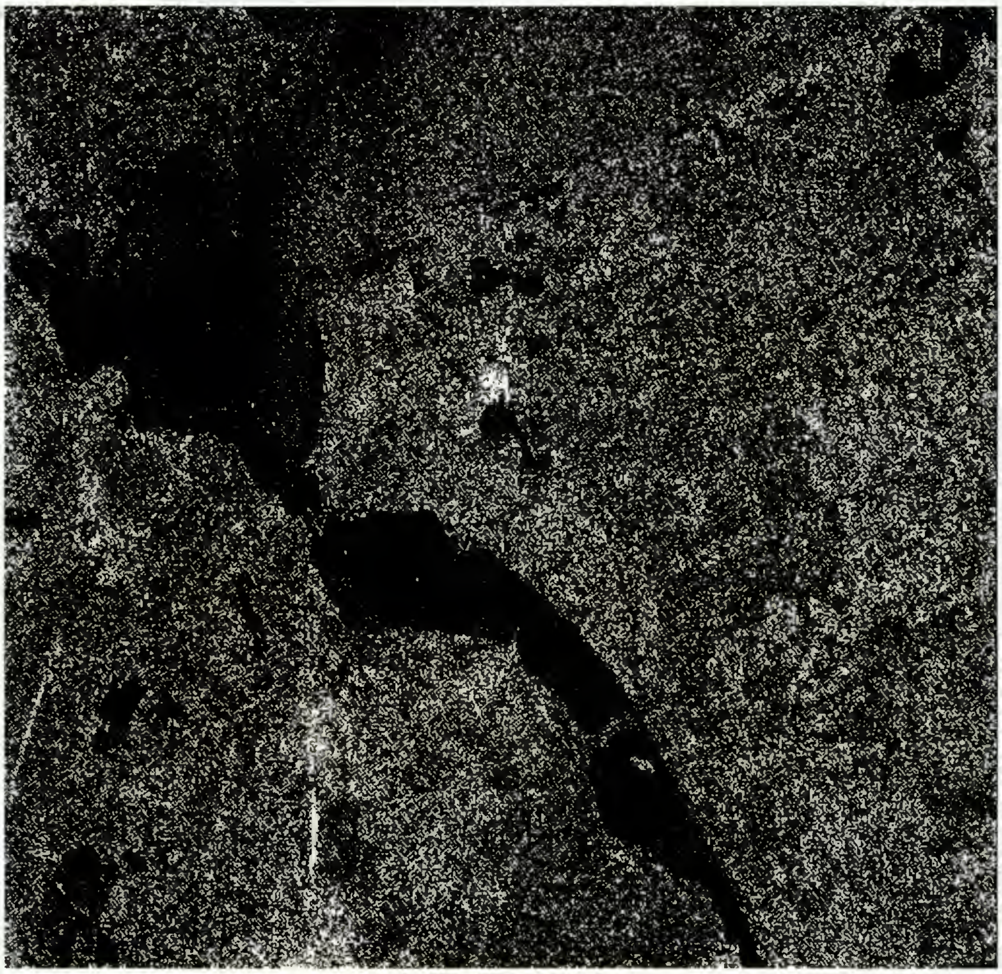

Image 5 Complex data to 1 Look simulated LR image, 10 September 1991, intensity.

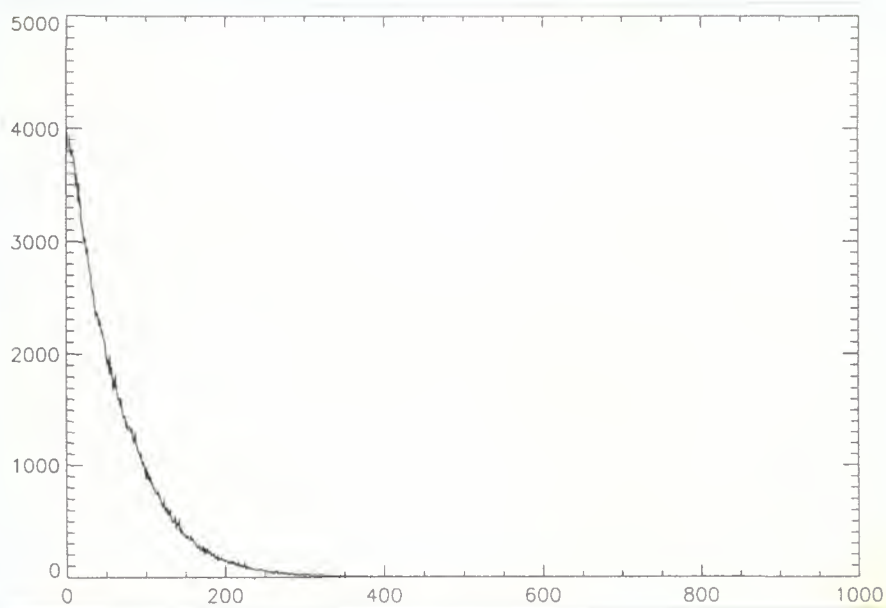

Figure 5.3 Histogram of Image 5.

5.1.4 8 Looks LR image (Image 6)

Simulation processing parameters :

	Comp. Integr.	Comp. B. Aver.	Moving W. Av.	Block Aver.
Range	3	3	2	1
Azimuth	6	6	4	2

LR image quality measurements :

Radiometric resolution :

Nominal Number of Looks :	8
Expected Equivalent Number of Looks :	5.6
Measured Equivalent Number of Looks :	***4.8***

Point target analysis :

Slant range pixel spac.	:	≅ 24 m	Azimuth pixel spacing	:	≅ 48 m
Measured ground range resolution	:	1.78 pixels ≅ 109 m	Measured azimuth resolution	:	1.67 pixels ≅ 80 m
Measured PSLR	:	15 dB			

The speckle reduction obtained with a nominal 8 looks LR image (about 5 effective looks) makes possible the distinction between fields, forests and built-up areas in image 6. The state of the sea surface can also be described. The transponder is difficult to find. Other details as roads and railways are more easily distinguished. The breakwater structure and land can be distinguished from the sea in the three dimensional plot of figure 5.4.

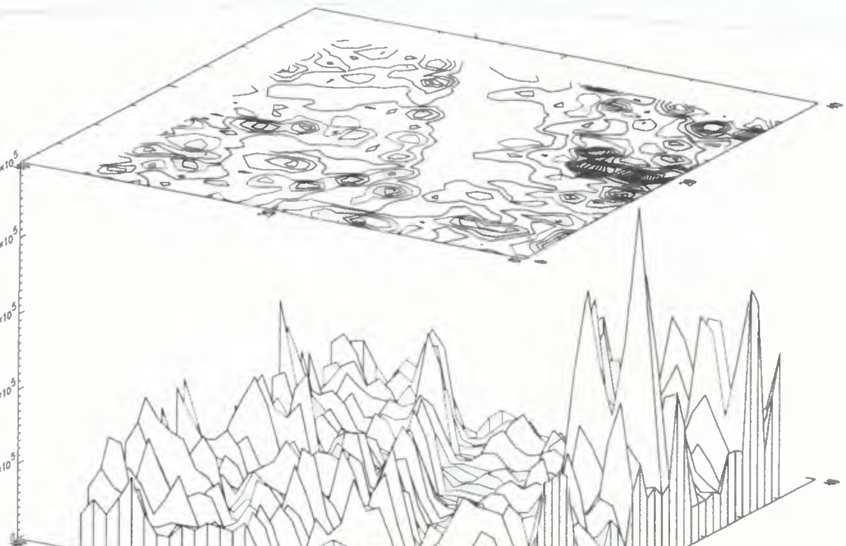

Figure 5.4 Three dimensional plot of breakwater structure for 8 looks LR image.

Image 6 Complex data to 8 Looks simulated LR image, 10 September 1991, intensity, 4.8 E.N.L.

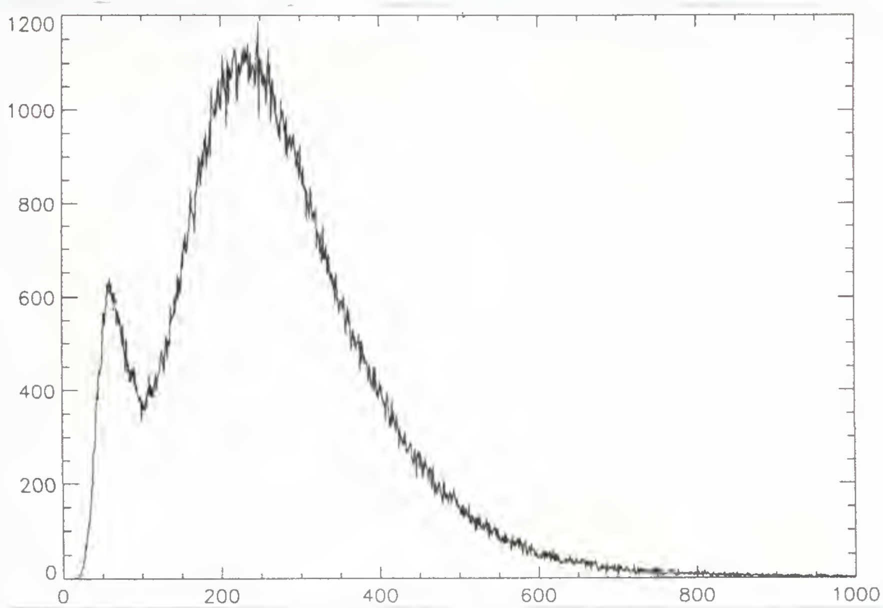

Figure 5.5 Histogram of Image 6.

5.1.5 16 looks LR image (Image 7)

Simulation processing parameters :

	Comp. Integr.	Comp. B. Aver.	Moving W. Av.	Block Aver.
Range	3	3	2	1
Azimuth	3	3	8	4

LR image quality measurements :

Radiometric resolution :

Nominal Number of Looks :	16
Expected Equivalent Number of Looks :	10.4
Measured Equivalent Number of Looks :	*9.3*

Point target analysis :

Slant range pixel spac.	:	≅ 24 m	Azimuth pixel spacing	:	≅ 48 m
Measured ground range resolution	:	1.84 pixels ≅ 113 m	Measured azimuth resolution	:	1.77 pixels ≅ 85 m
Measured PSLR	:	15 dB			

Comparing with the previous images, we have now a better distinction between the largest fields in the agricultural areas. Finer infrastructures are also visible; for example the road going south at the bottom left of the image. The breakwater structure and the land on the three dimensional plot of figure 5.8 are now easily distinguishable from the sea.

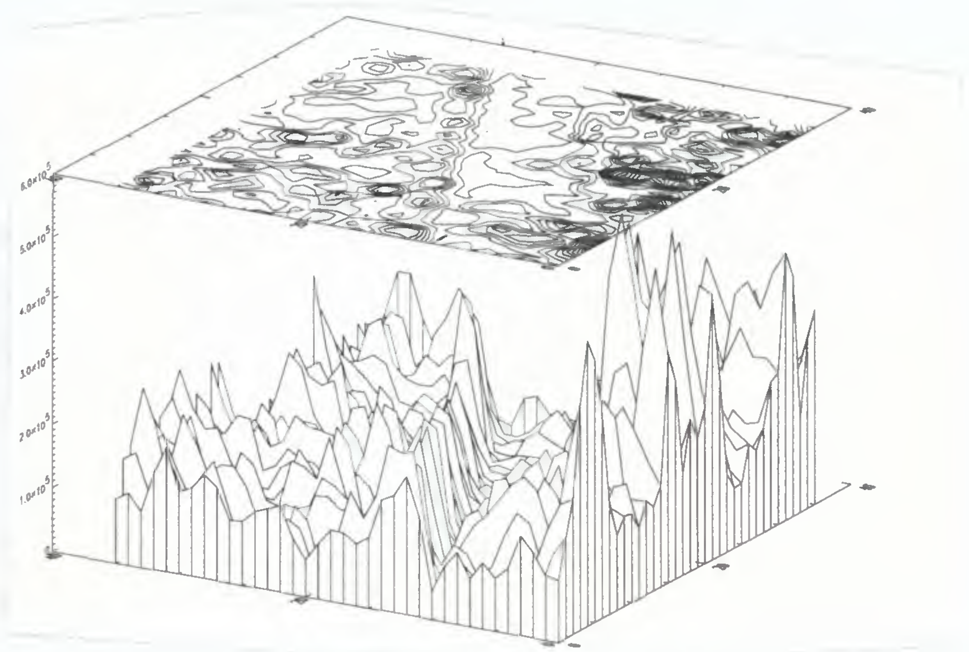

Figure 5.8 Three dimensional plot of breakwater structure for 16 look LR image.

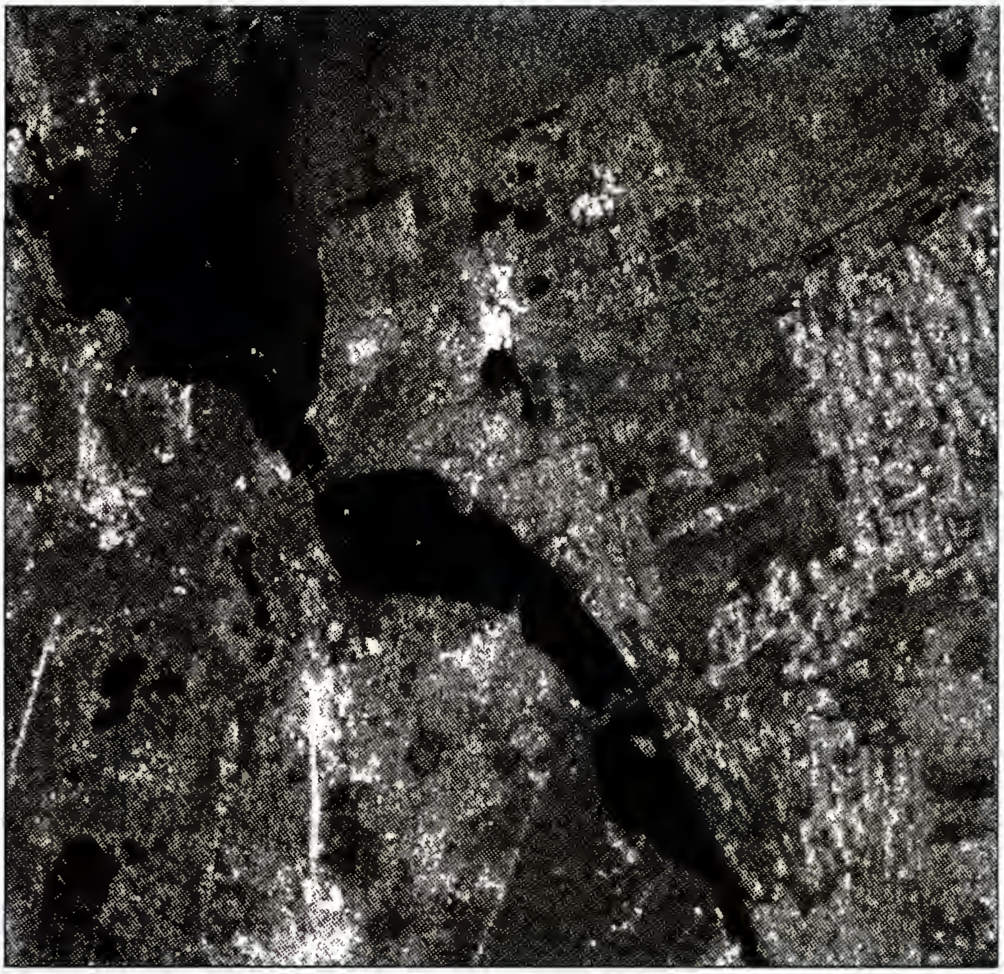

Image 7 Complex data to 16 Looks simulated LR image, 10 September 1991, intensity, 9.3 E.N.L.

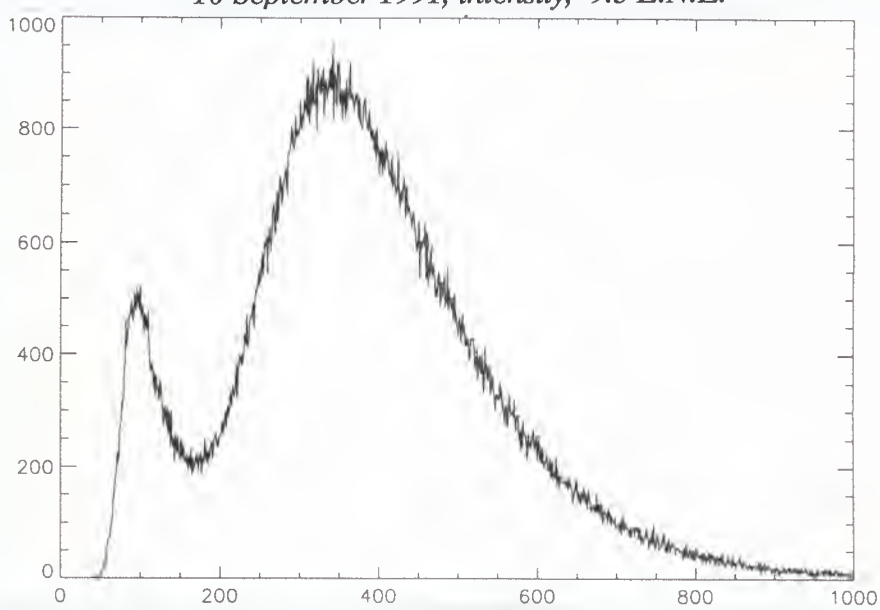

Figure 5.9 Histogram of Image 7.

5.1.6 48 Looks LR image (Image 8)

Simulation processing parameters :

	Comp. Integr.	Comp. B. Aver.	Moving W. Av.	Block Aver.
Range	1	1	6	3
Azimuth	3	3	8	4

LR image quality measurements :

Radiometric resolution :

Nominal Number of Looks :	48
Expected Equivalent Number of Looks :	31.0
Measured Equivalent Number of Looks :	*26.6*

Point target analysis :

Slant range pixel spac.	:	≅ 24 m	Azimuth pixel spacing	:	≅ 48 m
Measured ground range resolution	:	1.97 pixels ≅ 121 m	Measured azimuth resolution	:	1.76 pixels ≅ 84 m
Measured PSLR	:	15 dB			

In this image the speckle is so much reduced that a single pixel value can, potentially, be interpreted directly in relation to the backscattering coefficient of the surface, with an acceptable degree of error on the estimate. The finer infrastructure is still more clearly distinguished than in images 5, 6 and 7. The three dimensional plot of the breakwater structure confirms this in figure 5.10.

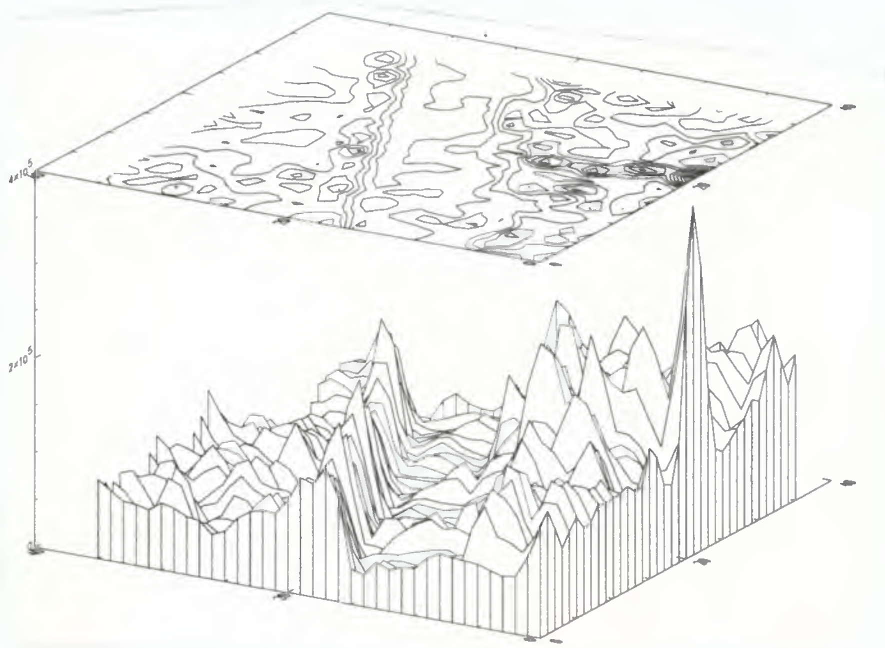

Figure 5.10 Three dimensional plot of breakwater structure for 48 looks LR image.

Image 8 Complex data to 48 Looks simulated LR image, 10 September 1991, intensity, 26.6 E.N.L.

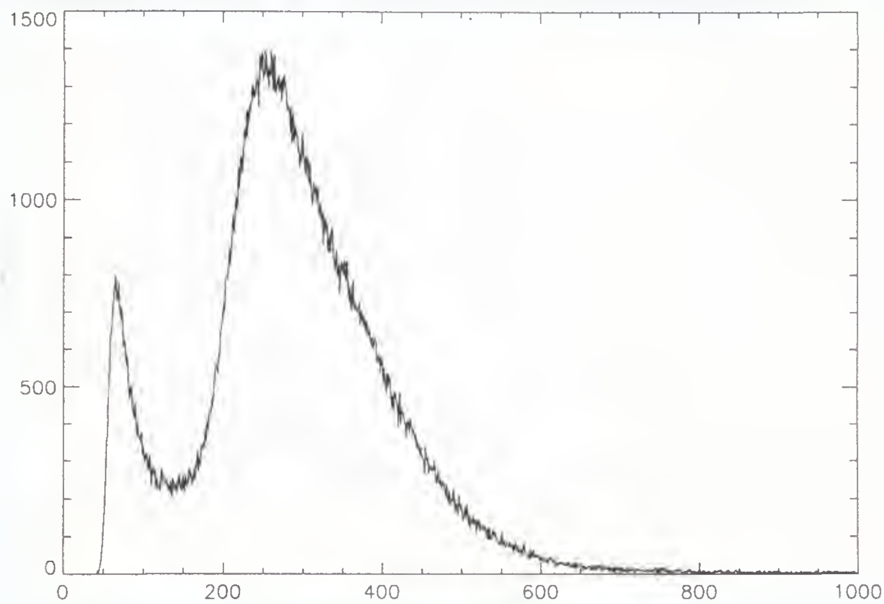

Figure 5.11 Histogram of Image 8.

5.1.7 156 Looks LR image (Image 9)

Simulation processing parameters :

	Comp. Integr.	Comp. B. Aver.	Moving W. Av.	Block Aver.
Range	1	1	6	3
Azimuth	1	1	26	13

LR image quality measurements :

Radiometric resolution :

Nominal Number of Looks :	156
Expected Equivalent Number of Looks :	127.4
Measured Equivalent Number of Looks :	***120.0***

Point target analysis :

Slant range pixel spac.	:	≅ 24 m	Azimuth pixel spacing	:	≅ 52 m
Measured ground range resolution	:	1.95 pixels ≅ 120 m	Measured azimuth resolution	:	2.03 pixels ≅ 106 m

Measured PSLR	:	15 dB

This image has the best radiometric resolution (0.38 dB) achievable using moving window averaging and block averaging for the chosen spatial resolution (100 m). This high number of looks means that a single pixel value in the resulting LR image can give directly the backscattering coefficient σ^0 of the analysed area. Details in the image are quite clear and different types of fields are easy to distinguish. The railways are now seen as continuos bright lines. The three dimensional plot of the breakwater structure area shows even greater radiometric difference between the different types of backscattering (figure 5.12).

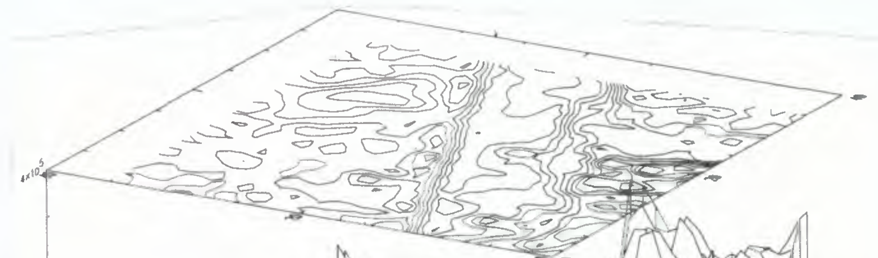

Figure 5.12 Three dimensional plot of breakwater structure for 156 looks LR image.

Image 9 Complex data to 156 Looks simulated LR image, 10 September 1991, intensity, 120 E.N.L.

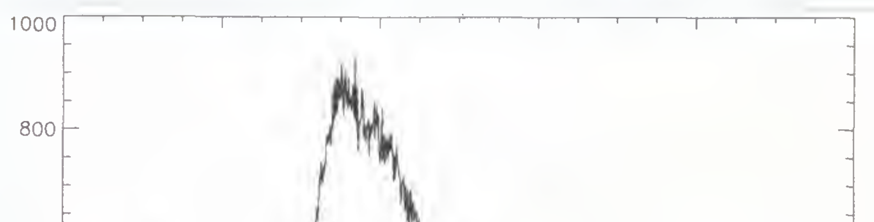

Figure 5.13 Histogram of Image 9.

5.2 HR DETECTED DATA TO 100 METRES RESOLUTION IMAGE

In the second part of our simulation study, we used HR detected data (UI16) to simulate a LR image with spatial resolutions of about 100 m (see section 2.2).

5.2.1 Description of the Detected Data used in the Simulation

The HR detected data used in the simulation cover the same area than the complex data used previously, but are acquired at a different date : 13 October 1991. This can easily be seen in the image by the changes in the wind patterns on the water surface. The detected image used is an UI16 product (see section 3.1)

5.2.2 The Method

The simulated image is generated using the following process (see section 2.2) :

Moving Window Averaging → Block Averaging

5.2.3 108 Looks LR image (Image 10)

Simulation processing parameters :

	Comp. Integr.	Comp. B. Aver.	Moving W. Av.	Block Aver.
Range	N/A	N/A	6	3
Azimuth	N/A	N/A	6	3

LR image quality measurements :

Radiometric resolution :

Nominal Number of Looks :	108
Expected Equivalent Number of Looks :	44
Measured Equivalent Number of Looks :	35

Point target analysis :

Ground range pixel spac.	:	≅ 60 m	Azimuth pixel spacing	:	≅ 48 m
Measured ground range resolution	:	1.99 pixels ≅ 119 m	Measured azimuth resolution	:	1.81 pixels ≅ 87 m
Measured PSLR	:	12 dB			

The expected equivalent number of looks is computed by using a spatial resolution of 28 m in range by 25 m in azimuth for the UI16.

In order to make comparisons with the simulated LR images of the previous section, we do an appropriate choice of moving window averaging and block averaging kernels. It should be noticed that these kernels are different from the ones chosen for the UILR product improvement (see section 3.1), the goal being not the same.

Because of the different acquisition dates of the HR data used in the simulation (HR complex data : 10 September 1991, HR detected data : 13 October 1991), the resulting LR images are different. For example the lack of calm water in the detected data derived LR image results in a differently shaped histogram. One should also note that the mean level of the detected data derived LR image is lower than the complex data derived LR images.

Comparing this product with the HR complex data derived images it is apparent that poorer radiometric resolution is obtained for the same spatial resolution. This is probably because the Doppler bandwidth used to generate the original HR detected product (960 Hz) is smaller than that used to generate the HR complex data (1332 Hz). Output quality depends on input quality.

One can note that the breakwater structure pictured in figure 5.14 is comparable to figure 5.10. Similar speckle reduction is performed on both images. One should also notice that the breakwater structure itself comes out poorer in the HR detected data derived image. This can be understood by the east-west orientation of the breakwater structure and the different azimuth resolutions of the original data (25 m for the detected data and 5 m for the complex data).

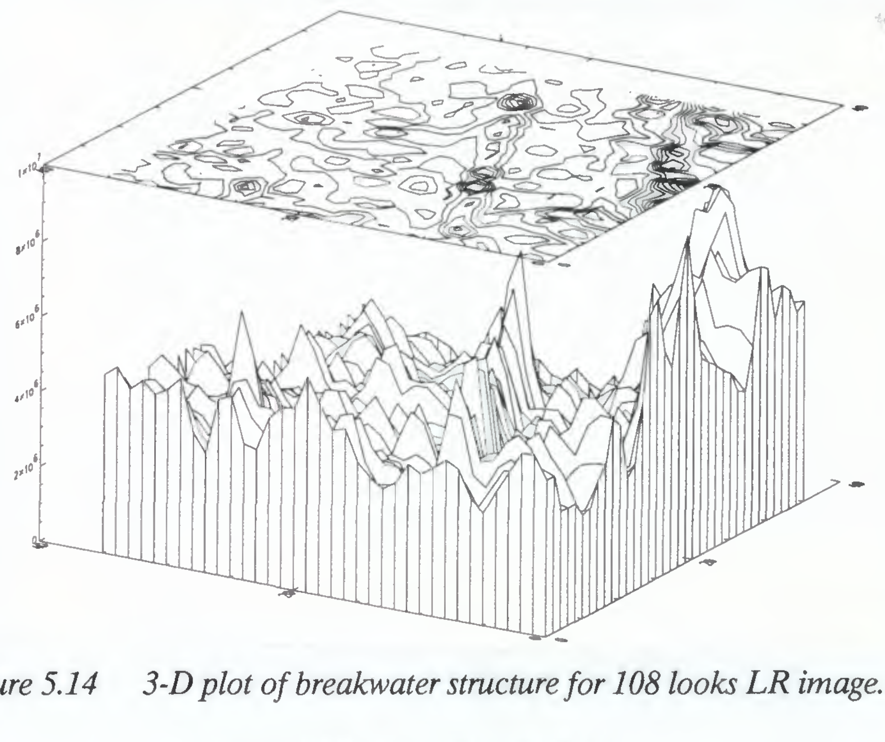

Figure 5.14 3-D plot of breakwater structure for 108 looks LR image.

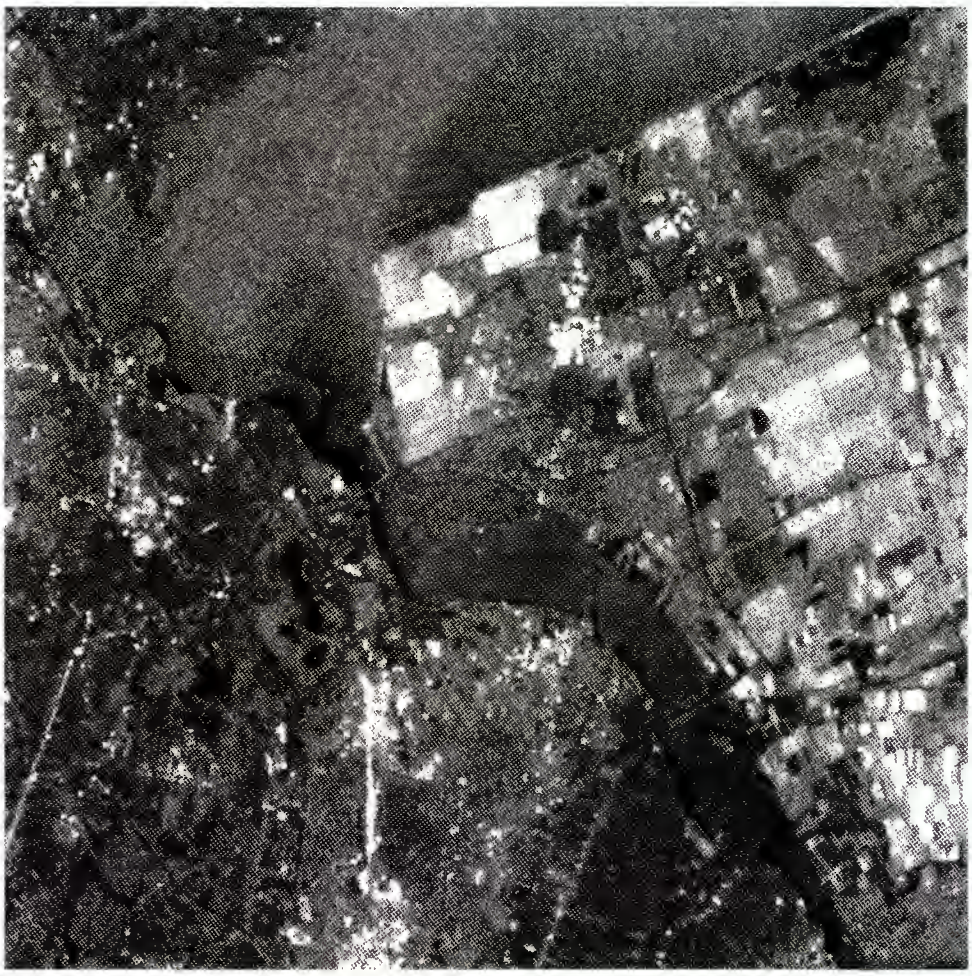

Image 10 *108 looks LR image from UI16, 13 October 1991, intensity.*

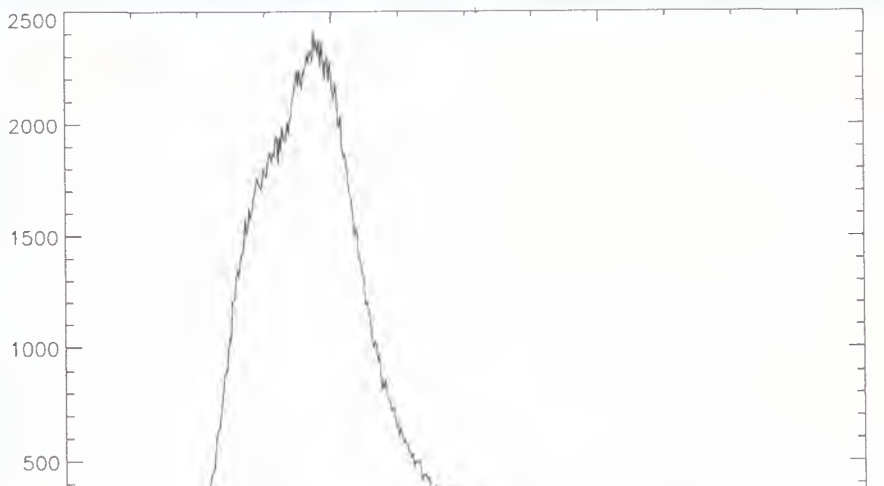

Figure 5.15 *Histogram of Image 10.*

5.3 HR Detected Data to 1 Kilometre Resolution Image

In the third part of our simulation study, we used HR detected data (UI16) to simulate LR images with spatial resolutions of about 1 km.
This study is done in the context of global scale SAR coverage where there is a potential interest in extreme large scale phenomena. With such a spatial resolution, the ERS swath contains between 100 and 200 pixels only.

5.3.1 Description of the Detected Data used in the Simulation

The HR detected data used in the simulation is an UI16 product covering the English Channel (La Manche) between Dover and Calais. This image has been chosen for its large scale wind and current patterns as well as for the balance between land and sea in the scene.

5.3.2 The Method

The simulated image is generated using the following process (see section 2.2) :

Integer Subsampling → Moving Window Averaging → Block Averaging

Simulation processing parameters :

	Subsampling	Moving W. Av.	Block Aver.
Range	1, 6, 12, 24, 24	50, 9, 5, 2, 1	25, 4, 2, 1, 1
Azimuth	1, 8, 16, 32, 32	64, 9, 5, 2, 1	32, 4, 2, 1, 1

The pixel spacing is brought down to 500 m by subsampling, low-pass filtering and block averaging. In all but the last image a spatial resolution of 1000 m is sought. We try to obtain square pixel sizes and spatial resolutions by applying greater azimuth sizes on the kernels.

5.3.3 Results (Images 11 to 15)

The first image ***(image 11)*** represents fully the bandwidth (960 Hz) of the original UI16 product since no subsampling is performed prior to the low pass filtering and

the block averaging. The quality of the image is very good (220 looks), and one can hardly tell it is a SAR image because of the lack of graininess.

At land one can distinguish densely inhabited areas from rural ones while at sea one can distinguish wind and current patterns.

The largest sea vessels are visible in the LR image as bright spots when the surrounding sea surface is relatively calm. In the original image one can distinguish strong backscattering both from the rough sea around and immediately behind the physical location of the vessel, and the vessel itself. The vessel is imaged with an azimuth displacement due to the Doppler shift introduced by the range speed of displacement. In the LR image these two sources of backscattering both fall into the same resolution cell, which can result in a distinct contrast from the surrounding sea.

The second image ***(image 12)*** is subsampled to change the radiometric resolution (now 60 looks) while keeping the same spatial resolution. The image is still interpretable as the first one, but a certain graininess can now be observed in the most homogenous parts of the sea. The image has lost its photographic quality and is more like a conventional SAR-image.

In the third image ***(image 13)*** the subsampling ratio is increased to introduce an even more severe reduction of radiometric resolution (44 looks). Now it becomes difficult to distinguish the sea from land and analysis will have to be based on statistics where one before could make use of single pixels with good precision.

In the fourth image ***(image 14)*** the radiometric resolution is considerably reduced (10 looks). The result is an image where information retrieval has become difficult because of the small size of the homogenous areas and the high speckle noise. Still some of the urban and agricultural areas can be identified.

For curiosity we have included an image ***(image 15)*** where only subsampling is performed. This gives a 3 look image (as the original UI16) with a spatial resolution close to one pixel (dependent on the scene). This image could only be used to verify the original image contents without data analysis. Very little information of the scene can meaningfully be extracted.

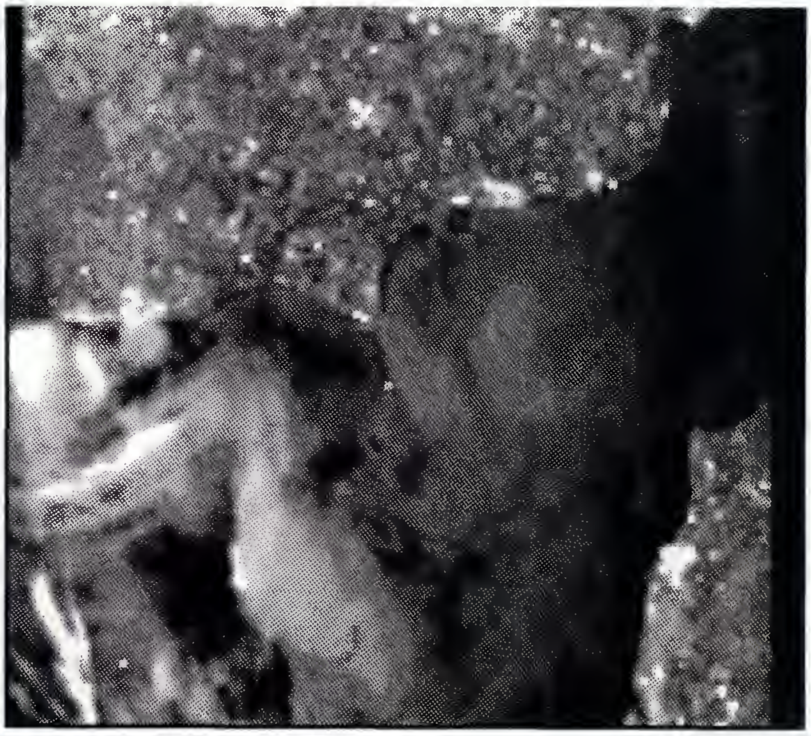

Image 11 220 Looks LR image, one kilometer resolution.

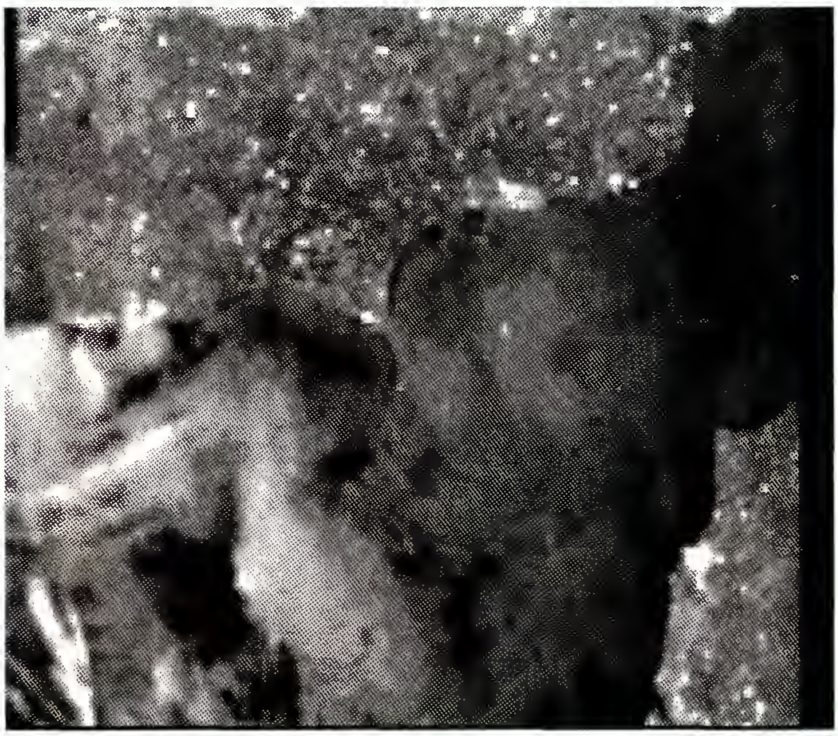

Image 12 60 Looks LR image, one kilometer resolution.

51

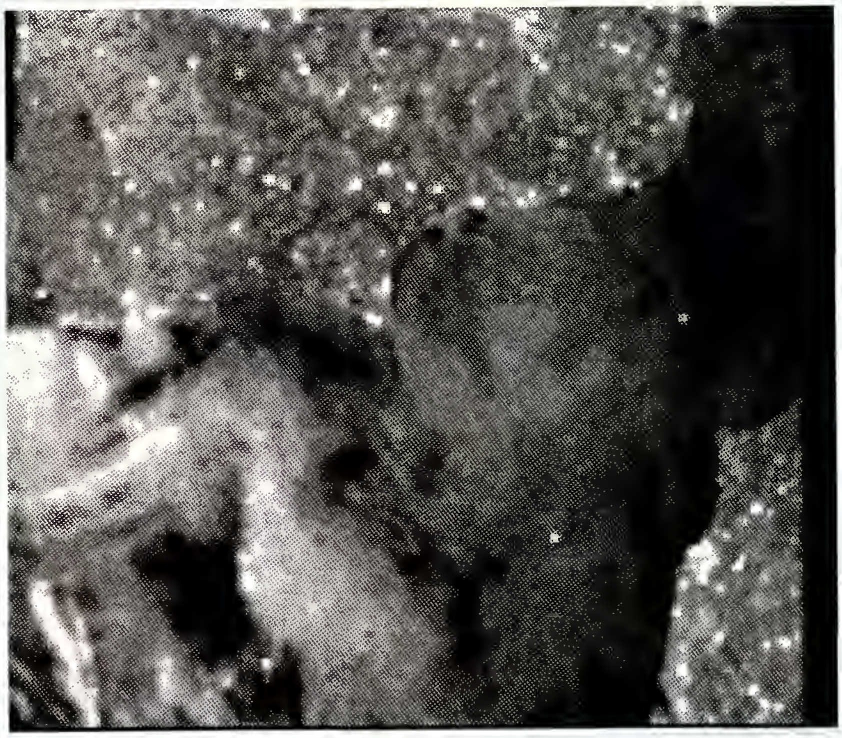

Image 13 *44 Looks LR image, one kilometer resolution.*

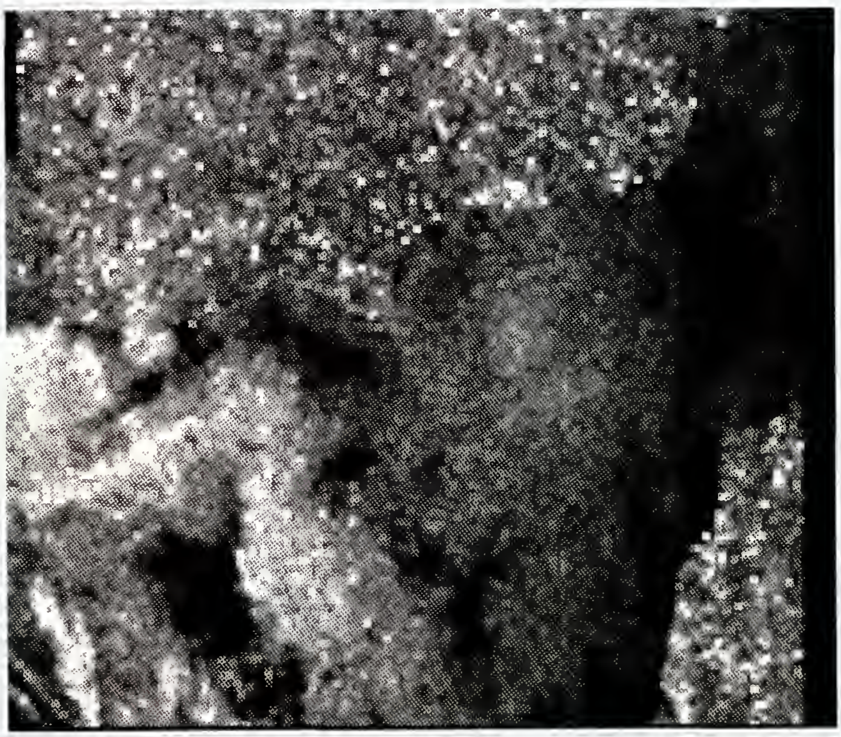

Image 14 *10 Looks LR image, one kilometer resolution.*

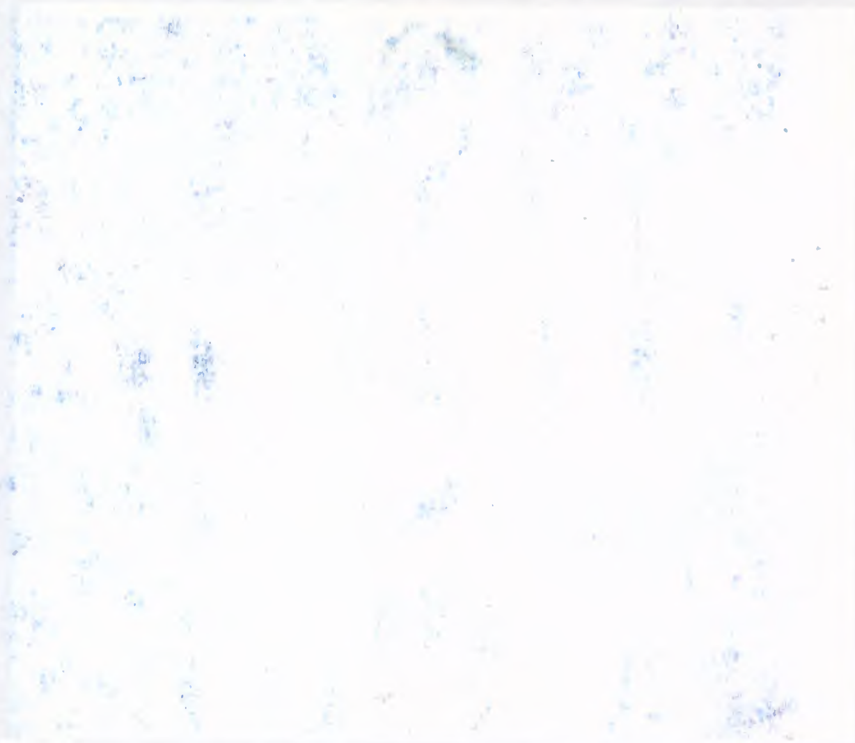

Image 15 3 Looks LR image, one kilometer resolution.

6 CONCLUSIONS

ERS low resolution SAR imagery has two origins :

- **derived from high resolution products**
- **derived directly from raw data**

ERS low resolution SAR imagery serves two goals :

- **digital product for scientific applications**
- **display for browse, raw data visualization or for request of HR production**

In our study, we have described and analysed the existing ERS-1 SAR Low Resolution imagery (see next table). We have proposed improvements to the quality of some of the analysed images.

EXISTING ERS-1 SAR LOW RESOLUTION IMAGERY		ORIGINS	
		DERIVED FROM HR PRODUCT	DERIVED FROM RAW DATA
GOALS	LR DIGITAL PRODUCT	• LRI Tromsø • SGC Gatineau • Lo-Res Fairbanks	**Future**
	DISPLAY / BROWSE	• UILR Kiruna	• QL Bangkok • QL Brazil • QL Antarctica

54

Given the two distinctive (and potentially conflicting) goals, ERS low resolution SAR imagery should meet the following criteria :

SAR LOW RESOLUTION IMAGERY		
CRITERION	**DIGITAL PRODUCT**	**DISPLAY / BROWSE**
1. To have a good radiometric resolution	Mandatory : better than 0.75 dB, i.e. > 28 E.N. Looks Recommended : better than 0.5 dB, i.e. > 70 E.N. Looks	Recommended : better than 1 dB, i.e. > 15 E.N. Looks
2. To be relatively and absolutely calibrated	Mandatory : relative calibration (for inter-comparison) Recommended : absolute calibration (for derivation of σ^o)	Not required
3. To have uniformly spaced pixels to limit geographic distortion [in order to avoid resampling]	Mandatory : less than 5 % difference between range and azimuth pixel spacing	Not required
4. To have a reduced data volume to allow swift and inexpensive transmission and to facilitate archiving	Mandatory : presentation : • ground range • amplitude, 8 bits • pixel spacing = 100 m	Mandatory : presentation : • amplitude, 8 bits • pixel spacing = 100 m Recommended : • data compression techniques • pixel spac. up to 200 m
5. To cover 100 % of the acquired raw data	Recommended	Mandatory
6. To be shortly available after data acquisition to allow real or near real time applications	Recommended : processing time better than 1/8th real time	Mandatory : processing time better than 1/8th real time
7. To have a good contrast enhancement	Not required	Recommended

Comments on the criteria

1. Good radiometric resolution

In the simulation of different radiometric resolutions for a fixed spatial resolution (chapter 5), we demonstrate (visually) that the better the radiometric resolution is, the easier the interpretation of the LR images is.
When the LR product is generated from HR product, a low pass filtering applied before the block averaging greatly improves the radiometric resolution of the LR product (section 2.2 and 3.1.3).

2. Relative and absolute calibration

Relative calibration (image-to-image)

LR digital products of the same area but of different acquisition times should be immediately comparable (without further processing). The radiometric stability measured on LR products should be identical to the one measured on high resolution products (for ERS-1, better than 0.5 dB).
In sections 2.3 and 3.1.1, we have presented two methods for 16 to 8 bit conversion of HR products. The fixed ratio conversion should be used because it does not affect the original radiometry.

Relative calibration (within one image)

LR digital products should be compensated for the antenna pattern and range spreading loss.

Absolute calibration

It should be possible to retrieve the backscattering coefficient σ^o in LR digital products:

$$\sigma^o = I / K$$

where K is the calibration constant of the LR product and I the intensity of few pixels (mean of the square of pixel values). If the LR product has more than 100 equivalent looks, the intensity I can be directly given by the square of <u>one</u> pixel value only.

3. Uniformly spaced pixels

This is necessary to avoid geographic distortion harmful to objects dynamics analysis in multi temporal LR products (e.g. sea ice movements).

4. Reduced data volume

In section 2.3, we have shown that the dynamic range of backscattering coefficients in ERS SAR images is completely contained in 8 bits. The pixel spacing should be 100 m and the spatial resolution about 150 m.
Previous presentation parameters give a typical size of 1 Mbyte for a LR digital product.
With pixel spacing of 200 m and use of data compression techniques, one can obtain LR imagery suitable for display purpose with a data volume of about 100 Kbytes per standard frame.

5. All acquisitions processed at Low Resolution

This criterion is particularly stringent for ground stations acquiring a large volume of raw data like the ESA Kiruna station (about 60 minutes of data per day). For such ground stations, the produced LR imagery should respect the next criteria.

6. Shortly available

For real or near real time applications, the LR imagery should be processed at near real-time (i.e. better than $1/8^{th}$ real time).

7. Good contrast enhancement

The contrast enhancement is only recommended for screen display purposes. In such a case, an algorithm based on the probability distribution can be applied on the image for contrast stretching (section 2.3).

SAR Low Resolution Imagery Evolution

The Figure 6.1 gives an overview of the current status and the evolution of ERS SAR Low Resolution imagery.

The ***existing*** LR imagery derived from raw data is able to provide ***visualization of all SAR acquisitions*** albeit with degraded image quality (case of Bangkok QL).

The ***existing*** LR imagery derived from HR products is able to provide ***LR digital products*** for scientific applications (case of Norwegian LRI product) but is far from covering all SAR acquisitions. At near term the quality of such LR digital products can be improved to better satisfy user needs.

The ***future*** LR imagery should be able to provide ***LR digital product with high image quality of all SAR acquisitions***. This goal is reachable if increased computer power is available.

Increased computer power means reduction of HR processing time, i.e. possibility to have HR products of all SAR acquisitions (and by consequence LR products of all SAR acquisitions). But in such a scenario one would have ***to drastically increase the archiving capacities of HR products***.

Increased computer power means quality improvement in LR imagery derived from raw data and by consequence possibility to have LR digital products with a good image quality. However in such a scenario, there would be the need to ***reprocess the data for HR products generation***.

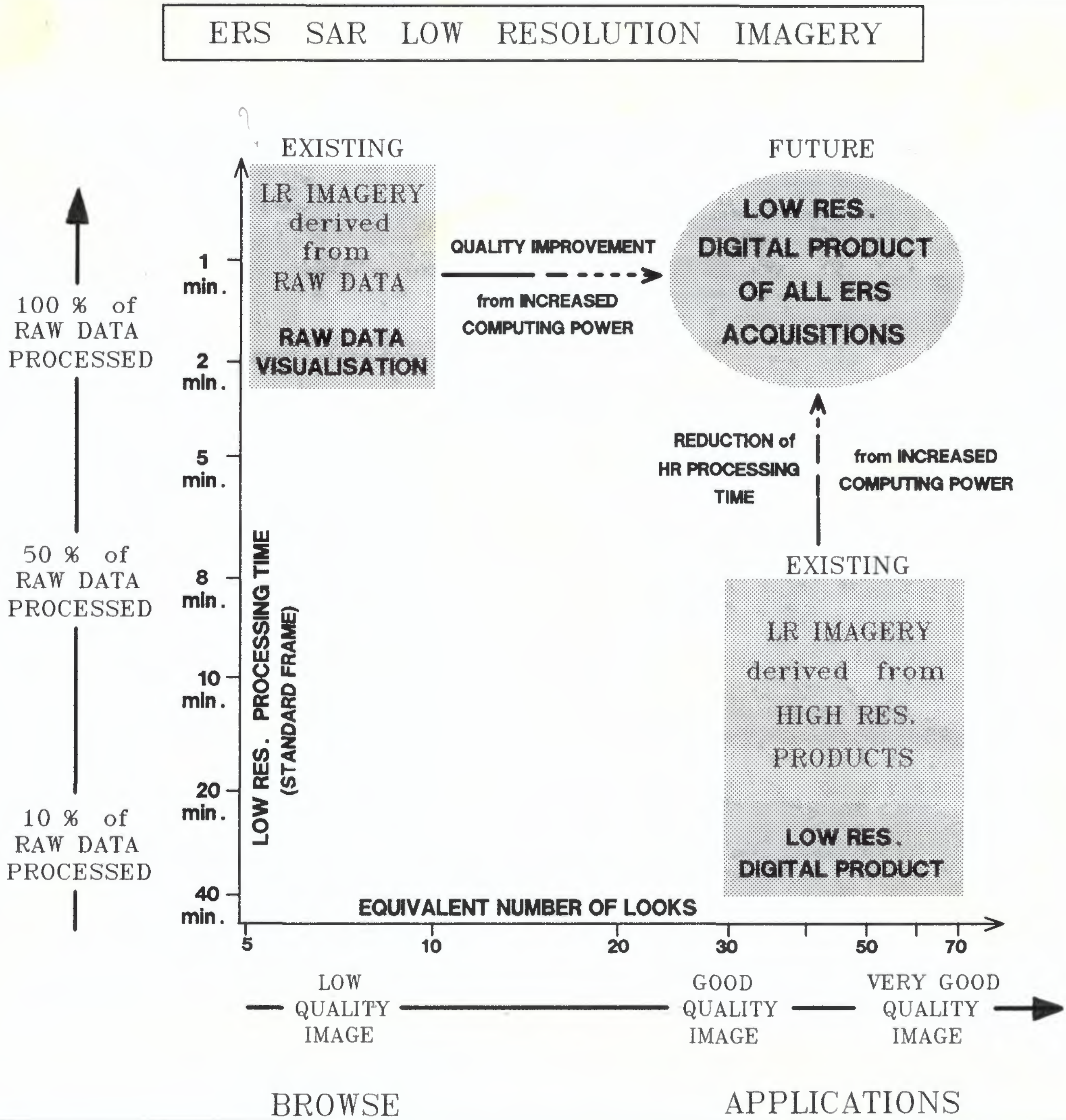

Figure 6.1 : Current status and evolution of the SAR Low Resolution imagery (see comments on the left)

7 REFERENCES

1. **European Space Agency,** "ERS-1 SAR Products Specification", ESA/ESRIN, Ref. SP-1149, June 1992.

2. **R. Touzi, K. Raney, A. Lopes,** "On the Use of Complex SAR Data for Calibration", Proc. of IGARSS'92 Symposium, IEEE 92CH3041-1, Vol. 2, pp. 1155 - 1157, May 1992.

3. **G. Aa. Solaas,** "Prètraitement des images radar á synthése d'ouverture", Study project for the Norwegian Institute of Technology, Electronics Department, Trondheim, Norway, Spring 1992.

4. **J. L. Marchand, J. R. Guasch,** "Data Compression Study for ERS-1 UILR Images", ESA/ESTEC, Ref. WDP/JLM/1859, 10 March 1993.

5. **I. Petiteville, C. Caspar,** "ERS-1 SAR Low Resolution Product Specification", ESA/ESTEC, Ref. ER-TN-ESA-GS-0207, Issue 1.3, 1 Feb. 1993.

6. **Tromsø Satellite Station,** "ERS-1 SAR Product Specification", issue 1/0, 9 Jul. 1991.

7. **MacDonald Dettwiler,** "Canadian Radar Data Centre, ERS-1 Data Processing Facility Product Specification", Ref. CE-IS-MDA-SY-0200, Issue/Revision 5/0, 29 Nov. 1990.

8. **D. Cuddy, M. Chen, T. Bicknell,** "Alaska SAR Processor Implementation for E-ERS-1", Proc. of IGARSS'92 Symposium, Vol. 1, pp. 599-602, May 1992.

9. **MacDonald Dettwiler,** Product Specifications for the Brazil INPE ERS-1 Ground Station", Ref. BZ-IS-50-2520, Issue/Revision 2/5, 18 Nov. 1991.

10. **Dornier**, "Dornier Advanced Real Time SAR Processor for Satellite Borne SAR Systems", Aug. 1991.

11. **A.P. Wolframm, G. Christen**, "Fast Two Dimensional Digital Filtering for Payload Operations Monitoring, Final presentation of MBB study phase 2", ESA/ESOC, 14 May 1992.

12. **A. Monti Guarnieri, C. Prati, F. Rocca**, "Development and Implementation of an ERS-1 Quick-Look Algorithm", ESA/ESRIN Contract No. 8658/90/HGE-I, 15 Oct. 1992.

13. **H. Laur**, "Technical Note on the ECISAR Test Image", ESA/ESRIN, ER-TN-EPO-GP-1901, Issue 1/0, 9 Oct. 1990.

14. **H. Laur**, "ECISAR Test Image, Quality Analysis and Calibration Measurements", ESA/ESRIN, ER-TN-EPO-GP-1902, Issue 1/1, 14 Jan. 1991.